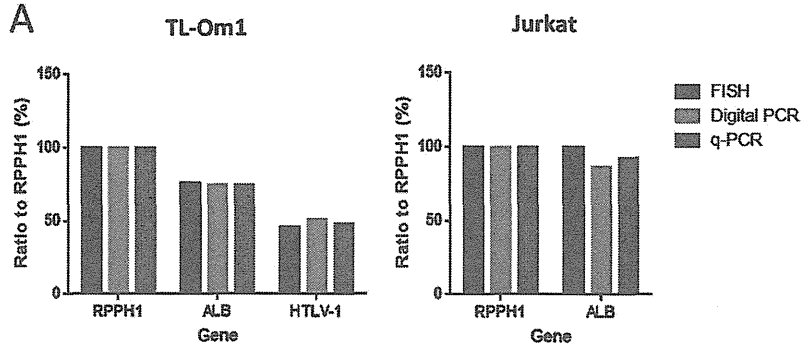

FIG 6 HTLV-1- and ALB-to-RPPH1 gene copy number ratios. (A) Comparison of the HTLV-1- and ALB-to-RPPH1 gene copy number ratios determined by FISH, digital PCR, and qPCR. Data indicate percentages of gene copy number ratio to the RPPH1 gene.

formed. Among the HTLV-1 cell lines, TL-Om1 is well known to be latently infected with HTLV-1 and is thought to be stable for HTLV-1 clonality (17, 26). Transcription from HTLV-1 provirus in TL-Om1 cells is blocked by the highly methylated LTR (27).

In this study, we evaluated the distinct genomic properties of HTLV-1 and IC genes in TL-Om1 cells with regard to their suitability as reference materials for HTLV-1 NATs. Precise information about HTLV-1 infectivity, karyotype, and absolute copy number of HTLV-1 and cellular control genes of TL-Om1 is useful for applying TL-Om1 as a reference material for HTLV-1 qPCR. As such, for this use, TL-Om1 has advantages over other cell lines, such as the human ATL cell line MT2 and the rat T-cell line TARL-2. A recent study of HTLV-1 testing in Japanese blood donor screening revealed that virus prevalence is not limited to areas where HTLV-1 is endemic but has shifted to the entire country, especially the Tokyo metropolitan area (6). Nationwide HTLV-1 tests have been performed on pregnant women in Japan since the end of 2010. The frequent occurrence of seroindeterminate results after Western blotting is one weakness of the HTLV-1 antibody tests. HTLV-1 qPCR is thought to be a solution for decreasing the number of seroindeterminate results; therefore, an accurate measurement of HTLV-1 proviral DNA by qPCR is needed. Additionally, a PVL value of >4% in PBMCs is reported to be a risk factor for ATL development from HTLV-1 asymptomatic carriers, which emphasizes the importance of measuring PVL by qPCR (7). PVL monitoring also provides a risk indicator for HAM/TSP (8).

An attempt to minimize the differences between laboratories by using a common plasmid that included the pX region has been reported. When standard curves were constructed by utilizing the common plasmid in all participating laboratories, the differences in median intralaboratory coefficient of variation (CV) could be reduced by about half (16). Although the attempt worked well among participating laboratories with in-house qPCR methods, the transferability of utilizing common plasmids for standard curves to other methods for PVL determination, for example, digital PCR, is uncertain.

To standardize HTLV-1 qPCR, we advocate the use of TL-Om1 cells with finely elucidated HTLV-1 genomic information as reference material. A previous report showed that PVL values of males and females, on average, are 1.39% and 2.10%, respectively (7). Thus, a dilution or a serial dilution of TL-Om1 with PBMCs or Jurkat cells at a PVL value of around 2% would be an appropriate material for the standardization of HTLV-1 qPCR. These kinds of references can be easily prepared, because the absolute gene copy number is determined from the dilution rate of TL-Om1. TL-Om1 cells were also used as a control in a deep-sequencing-based method for the quantification of the clone size of HTLV-1-infected cells in HTLV-1 carrier or ATL patients (28).

We conclude that TL-Om1 cells can be used as a useful reference material for HTLV-1 NATs. By using TL-Om1 cells, researchers will be able to define the exact values of HTLV-1 by quantifying the copy numbers of provirus and IC genes. In the future, we hope that other laboratories will utilize the features of TL-Om1 cells to standardize the HTLV-1 qPCR.

ACKNOWLEDGMENTS

This work was supported by grants-in-aid for scientific research and by Health and Labor Sciences research grant H23-shinkou-ippan-016 from the Ministry of Health, Labor and Welfare of Japan.

We thank all the members of the HTLV-1 qPCR standardization group for their useful discussions about this research.

We declare that we do not have any competing interests.

Ethical approval was not required for this study.

REFERENCES

1. Hinuma Y, Nagata K, Hanaoka M, Nakai M, Matsumoto T, Kinoshita KI, Shirakawa S, Miyoshi I. 1981. Adult T-cell leukemia: antigen in an ATL cell line and detection of antibodies to the antigen in human sera. Proc Natl Acad Sci U S A 78:6476–6480. http://dx.doi.org/10.1073/pnas.78.10.6476.
2. Poiesz BJ, Ruscetti FW, Gazdar AF, Bunn PA, Minna JD, Gallo RC. 1980. Detection and isolation of type C retrovirus particles from fresh and cultured lymphocytes of a patient with cutaneous T-cell lymphoma. Proc Natl Acad Sci U S A 77:7415–7419. http://dx.doi.org/10.1073/pnas.77.12.7415.
3. Watanabe T. 1997. HTLV-1-associated diseases. Int J Hematol 66:257–278. http://dx.doi.org/10.1016/S0925-5710(97)00077-7.
4. Gessain A, Cassar O. 2012. Epidemiological aspects and world distribution of HTLV-1 infection. Front Microbiol 3:388. http://dx.doi.org/10.3389/fmicb.2012.00388.
5. Watanabe T. 2011. Current status of HTLV-1 infection. Int J Hematol 94:430–434. http://dx.doi.org/10.1007/s12185-011-0934-4.
6. Satake M, Yamaguchi K, Tadokoro K. 2012. Current prevalence of HTLV-1 in Japan as determined by screening of blood donors. J Med Virol 84:327–335. http://dx.doi.org/10.1002/jmv.23181.
7. Iwanaga M, Watanabe T, Utsunomiya A, Okayama A, Uchimaru K, Koh KR, Ogata M, Kikuchi H, Sagara Y, Uozumi K, Mochizuki M, Tsukasaki K, Saburi Y, Yamamura M, Tanaka J, Moriuchi Y, Hino S, Kamihira S, Yamaguchi K, Joint Study on Predisposing Factors of ATLDi. 2010. Human T-cell leukemia virus type I (HTLV-1) proviral load

and disease progression in asymptomatic HTLV-1 carriers: a nationwide prospective study in Japan. Blood **116**:1211–1219. http://dx.doi.org/10.1182/blood-2009-12-257410.

8. **Takenouchi N, Yamano Y, Usuku K, Osame M, Izumo S.** 2003. Usefulness of proviral load measurement for monitoring of disease activity in individual patients with human T-lymphotropic virus type I-associated myelopathy/tropical spastic paraparesis. J Neurovirol **9**:29–35. http://dx.doi.org/10.1080/13550280390173418.
9. **Costa JM, Segurado AC.** 2009. Molecular evidence of human T-cell lymphotropic virus types 1 and 2 (HTLV-1 and HTLV-2) infections in HTLV seroindeterminate individuals from Sao Paulo, Brazil. J Clin Virol **44**:185–189. http://dx.doi.org/10.1016/j.jcv.2008.12.015.
10. **Zanjani DS, Shahabi M, Talaei N, Afzalaghaee M, Tehranian F, Bazargani R.** 2011. Molecular analysis of human T cell lymphotropic virus type 1 and 2 (HTLV-1/2) seroindeterminate blood donors from Northeast Iran: evidence of proviral *tax*, *env*, and *gag* sequences. AIDS Res Hum Retroviruses **27**:131–135. http://dx.doi.org/10.1089/aid.2010.0017.
11. **Watanabe M, Ohsugi T, Shoda M, Ishida T, Aizawa S, Maruyama-Nagai M, Utsunomiya A, Koga S, Yamada Y, Kamihira S, Okayama A, Kikuchi H, Uozumi K, Yamaguchi K, Higashihara M, Umezawa K, Watanabe T, Horie R.** 2005. Dual targeting of transformed and untransformed HTLV-1-infected T cells by DHMEQ, a potent and selective inhibitor of NF-kappaB, as a strategy for chemoprevention and therapy of adult T-cell leukemia. Blood **106**:2462–2471. http://dx.doi.org/10.1182/blood-2004-09-3646.
12. **Tanaka G, Okayama A, Watanabe T, Aizawa S, Stuver S, Mueller N, Hsieh CC, Tsubouchi H.** 2005. The clonal expansion of human T lymphotropic virus type 1-infected T cells: a comparison between seroconverters and long-term carriers. J Infect Dis **191**:1140–1147. http://dx.doi.org/10.1086/428625.
13. **Nagai M, Yamano Y, Brennan MB, Mora CA, Jacobson S.** 2001. Increased HTLV-I proviral load and preferential expansion of HTLV-I Tax-specific CD8+ T cells in cerebrospinal fluid from patients with HAM/TSP. Ann Neurol **50**:807–812. http://dx.doi.org/10.1002/ana.10065.
14. **Kamihira S, Dateki N, Sugahara K, Yamada Y, Tomonaga M, Maeda T, Tahara M.** 2000. Real-time polymerase chain reaction for quantification of HTLV-1 proviral load: application for analyzing aberrant integration of the proviral DNA in adult T-cell leukemia. Int J Hematol **72**:79–84.
15. **Ueno S, Umeki K, Takajo I, Nagatomo Y, Kusumoto N, Umekita K, Morishita K, Okayama A.** 2012. Proviral loads of human T-lymphotropic virus type 1 in asymptomatic carriers with different infection routes. Int J Cancer **130**:2318–2326. http://dx.doi.org/10.1002/ijc.26289.
16. **Kamihira S, Yamano Y, Iwanaga M, Sasaki D, Satake M, Okayama A, Umeki K, Kubota R, Izumo S, Yamaguchi K, Watanabe T.** 2010. Intra- and inter-laboratory variability in human T-cell leukemia virus type-1 proviral load quantification using real-time polymerase chain reaction assays: a multi-center study. Cancer Sci **101**:2361–2367. http://dx.doi.org/10.1111/j.1349-7006.2010.01720.x.
17. **Sugamura K, Fujii M, Kannagi M, Sakitani M, Takeuchi M, Hinuma Y.** 1984. Cell surface phenotypes and expression of viral antigens of various human cell lines carrying human T-cell leukemia virus. Int J Cancer **34**:221–228. http://dx.doi.org/10.1002/ijc.2910340213.
18. **Yoshida M, Seiki M, Yamaguchi K, Takatsuki K.** 1984. Monoclonal integration of human T-cell leukemia provirus in all primary tumors of adult T-cell leukemia suggests causative role of human T-cell leukemia virus in the disease. Proc Natl Acad Sci U S A **81**:2534–2537. http://dx.doi.org/10.1073/pnas.81.8.2534.
19. **Yamaguchi K, Seiki M, Yoshida M, Nishimura H, Kawano F, Takatsuki K.** 1984. The detection of human T cell leukemia virus proviral DNA and its application for classification and diagnosis of T cell malignancy. Blood **63**:1235–1240.
20. **Uren AG, Mikkers H, Kool J, van der Weyden L, Lund AH, Wilson CH, Rance R, Jonkers J, van Lohuizen M, Berns A, Adams DJ.** 2009. A high-throughput Splinkerette-PCR method for the isolation and sequencing of retroviral insertion sites. Nat Protoc **4**:789–798. http://dx.doi.org/10.1038/nprot.2009.64.
21. **Sanger F, Nicklen S, Coulson AR.** 1977. DNA sequencing with chain-terminating inhibitors. Proc Natl Acad Sci U S A **74**:5463–5467. http://dx.doi.org/10.1073/pnas.74.12.5463.
22. **World Health Organization.** 2011. International collaborative study to establish the 3rd WHO international standard for HIV-1 NAT assays. WHO ECBS report 2011 WHO/BS/2011.2178. WHO, Geneva, Switzerland.
23. **Fryer JF, Heath A, Wilkinson DE, Minor PD, The Collaborative Study Group.** 2011. Collaborative study to evaluate the proposed 3rd WHO international standard for hepatitis B virus (HBV) for nucleic acid amplification technology (NAT)-based assays. WHO ECBS report 2011 WHO/BS/2011.2170. WHO, Geneva, Switzerland.
24. **Fryer JF, Heath A, Wilkinson DE, Minor PD, The Collaborative Study Group.** 2011. Collaborative study to evaluate the proposed 4th WHO international standard for hepatitis C virus (HCV) for nucleic acid amplification technology (NAT)-based assays. WHO ECBS report 2011 WHO/BS/2011.2173. WHO, Geneva, Switzerland.
25. **White HE, Matejtschuk P, Rigsby P, Gabert J, Lin F, Lynn Wang Y, Branford S, Muller MC, Beaufils N, Beillard E, Colomer D, Dvorakova D, Ehrencrona H, Goh HG, El Housni H, Jones D, Kairisto V, Kamel-Reid S, Kim DW, Langabeer S, Ma ES, Press RD, Romeo G, Wang L, Zoi K, Hughes T, Saglio G, Hochhaus A, Goldman JM, Metcalfe P, Cross NC.** 2010. Establishment of the first World Health Organization international genetic reference panel for quantitation of BCR-ABL mRNA. Blood **116**:e111–e117. http://dx.doi.org/10.1182/blood-2010-06-291641.
26. **Koiwa T, Hamano-Usami A, Ishida T, Okayama A, Yamaguchi K, Kamihira S, Watanabe T.** 2002. 5′-Long terminal repeat-selective CpG methylation of latent human T-cell leukemia virus type 1 provirus *in vitro* and *in vivo*. J Virol **76**:9389–9397. http://dx.doi.org/10.1128/JVI.76.18.9389-9397.2002.
27. **Ishida T, Hamano A, Koiwa T, Watanabe T.** 2006. 5′ Long terminal repeat (LTR)-selective methylation of latently infected HIV-1 provirus that is demethylated by reactivation signals. Retrovirology **3**:69. http://dx.doi.org/10.1186/1742-4690-3-69.
28. **Firouzi S, Lopez Y, Suzuki Y, Nakai K, Sugano S, Yamochi T, Watanabe T.** 2014. Development and validation of a new high-throughput method to investigate the clonality of HTLV-1-infected cells based on provirus integration sites. Genome Med **6**:46. http://dx.doi.org/10.1186/gm568.

PLOS ONE

System Vaccinology for the Evaluation of Influenza Vaccine Safety by Multiplex Gene Detection of Novel Biomarkers in a Preclinical Study and Batch Release Test

Takuo Mizukami[1], Haruka Momose[1], Madoka Kuramitsu[1], Kazuya Takizawa[1], Kumiko Araki[1], Keiko Furuhata[1], Ken J. Ishii[2,3], Isao Hamaguchi[1]*, Kazunari Yamaguchi[1]

1 Laboratory of Blood and Vaccine safety, Department of Safety Research on Blood and Biologicals, National Institute of Infectious Diseases, Tokyo, Japan, **2** Laboratory of Adjuvant Innovation, National Institute of Biomedical Innovation (NIBIO), Osaka, Japan, **3** Laboratory of Vaccine Science, WPI Immunology Frontier Research Center (WPI-IFREC), Osaka University, Osaka, Japan

Abstract

Vaccines are beneficial and universal tools to prevent infectious disease. Thus, safety of vaccines is strictly evaluated in the preclinical phase of trials and every vaccine batch must be tested by the National Control Laboratories according to the guidelines published by each country. Despite many vaccine production platforms and methods, animal testing for safety evaluation is unchanged thus far. We recently developed a systems biological approach to vaccine safety evaluation where identification of specific biomarkers in a rat pre-clinical study evaluated the safety of vaccines for pandemic H5N1 influenza including *Irf7, Lgals9, Lgalsbp3, Cxcl11, Timp1, Tap2, Psmb9, Psme1, Tapbp, C2, Csf1, Mx2, Zbp1, Ifrd1, Trafd1, Cxcl9, β2m, Npc1, Ngfr* and *Ifi47*. The current study evaluated whether these 20 biomarkers could evaluate the safety, batch-to-batch and manufacturer-to-manufacturer consistency of seasonal trivalent influenza vaccine using a multiplex gene detection system. When we evaluated the influenza HA vaccine (HAv) from four different manufactures, the biomarker analysis correlated to findings from conventional animal use tests, such as abnormal toxicity test. In addition, sensitivity of toxicity detection and differences in HAvs were higher and more accurate than with conventional methods. Despite a slight decrease in body weight caused by HAv from manufacturer B that was not statistically significant, our results suggest that HAv from manufacturer B is significantly different than the other HAvs tested with regard to *Lgals3bp, Tapbp, Lgals9, Irf7* and *C2* gene expression in rat lungs. Using the biomarkers confirmed in this study, we predicted batch-to-batch consistency and safety of influenza vaccines within 2 days compared with the conventional safety test, which takes longer. These biomarkers will facilitate the future development of new influenza vaccines and provide an opportunity to develop *in vitro* methods of evaluating batch-to-batch consistency and vaccine safety as an alternative to animal testing.

Citation: Mizukami T, Momose H, Kuramitsu M, Takizawa K, Araki K, et al. (2014) System Vaccinology for the Evaluation of Influenza Vaccine Safety by Multiplex Gene Detection of Novel Biomarkers in a Preclinical Study and Batch Release Test. PLoS ONE 9(7): e101835. doi:10.1371/journal.pone.0101835

Editor: Sang-Moo Kang, Georgia State University, United States of America

Received March 10, 2014; **Accepted** June 11, 2014; **Published** July 10, 2014

Data Availability: The authors confirm that all data underlying the findings are fully available without restriction. All data are included within the paper.

Funding: This work was supported by Grants-in-Aid from Ministry of Health, Labor, and Welfare of Japan (201132001 and 201208036, respectively). The funders had no role in study design, data collection and analysis, decision to publish, or preparation of the manuscript.

Competing Interests: The authors have declared that no competing interests exist.

* Email: 130hama@nih.go.jp

Introduction

Vaccination is a beneficial and universal tool to prevent infectious disease [1]. Because most vaccines are derived from inactivated virus, bacteria or toxoids, contamination by incomplete inactivation can cause serious adverse events. Thus, historically, the safety of vaccines is strictly regulated by law and each batch of vaccine must be tested by the National Control Laboratories according to the guidelines published in each country, *e.g.* the European Pharmacopeia, United States Pharmacopeia and World Health Organization guidelines [2]. After the diphtheria toxoid (DT) immunization incident in Japan in 1950 that caused the death of 68 children and illness in over 600 infants owing to contamination by incomplete inactivation of DT [3], the abnormal toxicity test (ATT) (also known as general safety test) was introduced to the Japanese guidelines. This stated that the minimum requirement of biological products (MRBP) and all inactivated vaccines and toxoids was mandatory safety evaluation by ATT and other specific toxicity tests.

Influenza vaccine is one of the most widely used commercially available vaccines worldwide for preventing seasonal influenza and its complications. Influenza virus vaccine is mainly produced using embryonated fertilized chicken eggs and inactivated with formaldehyde. Whole particle influenza virus vaccine [WPv] was first licensed as an influenza vaccine in the US in 1945 [4] and is still used in some countries. Although WPv contains all the components of the influenza virus and induces strong immunity in the vaccinated individual, a high incidence of adverse events, including local reactions at the site of injection and febrile illness, particularly among children have been reported [5,6]. Thus, most recent vaccines manufactured since the 1970s have been subvirion vaccines. The subvirion influenza HA vaccine [HAv] showed a marked reduction of pyrogenicity compared with WPv [7]. The trivalent influenza vaccine [TIV] is a recently developed subvirion

influenza vaccine with components selected and updated each year to protect against one of the three main groups of circulating influenza virus strains in humans. TIV may be administered every year. Vaccine adjuvant, e.g. alum, MF59 and AS03, was also used to enhance immunity in preparation for the H5N1 pandemic [8]. To improve immunogenicity and reduce toxicity in addition to batch-to-batch quality assurance of influenza vaccine, seed lot systems, recombinant DNA technology, as well as animal and insect cell culture inactivated vaccine production systems were introduced. Despite the increase in many vaccine production platforms, adjuvants, additives and vaccine types, safety evaluation tests in the preclinical phase and batch release have been unchanged in most countries, including in Japan.

We previously reported that improved ATT could evaluate and assure the batch-to-batch consistency of vaccines more strictly compared with conventional methods [9]. In addition, we recently introduced a system biological approach to vaccine safety evaluation and demonstrated that specific biomarkers could be used to evaluate batch-to-batch consistency and safety of vaccines to diphtheria-pertussis-tetanus (DPT) [10,11] and Japanese encephalitis virus (JEV) [12]. Most recently, we showed that a system biological approach could evaluate the safety of pandemic H5N1 influenza vaccine [13]. We found 20 biomarkers for the evaluation of batch-to-batch consistency and the safety of H5N1 vaccine compared with HAv.

In this study, we tested whether these biomarkers could evaluate batch-to-batch consistency and the safety of seasonal HAv, as well as adjuvanted whole virion-derived influenza vaccine, using a multiplex gene detection system. This method might facilitate the evaluation of batch-to-batch consistency of HAv and reduce the time required for batch release compared with conventional ATT. These biomarkers will help the future development of new *in vitro* methods to evaluate vaccine safety as an alternative to animal testing.

Materials and Methods

1. Animals and Ethics statement

Eight-week-old male Fischer (F334/N) rats weighing 160–200 g were obtained from SLC (Tokyo, Japan). All animals were housed in rooms maintained at 23±1°C, with 50±10% relative humidity, and 12-h light/dark cycles for at least 1 week prior to the test use. All animal experiments were performed according to the guidelines of the Institutional Animal Care and Use Committee of the National Institute of Infectious Diseases (NIID), Tokyo, Japan. The study was approved by the Institutional Animal Care and Use Committee of NIID.

2. Vaccines

The following vaccines were used in this study: (1) PDv: inactivated monovalent A/H5N1 whole-virion influenza vaccine (derived from NIBRG-14: A/Vietnam/1194/2004) adjuvanted with aluminum hydroxide, containing 30 μg HA/ml; (2) WPv: inactivated whole trivalent influenza vaccine (A/Newcaledonia/20/99 (H1N1), A/Hiroshima/52/2005 (H3N2), and B/Malaysia/2506/2004); HAV: trivalent HA influenza vaccine (A/Solomon Island/3/2006 (H1N1), A/Hiroshima/52/2005 (H3N2), and B/Malaysia/2506/2004), containing 30 μg HA/ml each strain. For evaluation of commercially distributed HAV in Japan, we used trivalent HA influenza vaccine (A/Solomon Island/3/2006 (H1N1), A/Hiroshima/52/2005 (H3N2) and B/Malaysia/2506/2004), containing 30 μg HA/ml per strain. PDv and WPv were produced, and manufactured by the Chemo-Sero-Therapeutic Research Institute, Kaketsuken (Kumamoto, Japan). Licensed and authorized HAvs were purchased from four different manufactur-

Table 1. Biomarkers to evaluate influenza vaccine safety.

Official Symbol	Official Full Name	Gene ID
Irf7	Interferon regulatory factor 7	293624
Lgals9	Lectin, galactoside-binding, soluble, 9	25476
Lgalsbp3	Lectin, galactoside-binding, soluble, 3 binding protein	245955
Cxcl11	Chemokine (C-X-C motif) ligand 11	305236
Timp1	TIMP metallopeptidase inhibitor 1	116510
Tap2	Transporter 2, ATP-binding cassette, sub-family B	24812
Psmb9	Proteasome (prosome, macropain) subunit, beta type, 9	24967
Psme1	Proteasome (prosome, macropain) activator subunit 1	29630
Tapbp	TAP binding protein (tapasin)	25217
C2	Complement component 2	24231
Csf1	Colony stimulating factor 1 (macrophage)	78965
Mx2	Myxovirus (influenza virus) resistance 2	286918
Zbp1	Z-DNA binding protein 1	171091
Ifrd1	Interferon-related developmental regulator 1	29596
Trafd1	TRAF type zinc finger domain containing 1	114635
Cxcl9	Chemokine (C-X-C motif) ligand 9	246759
β2m	Beta-2 microglobulin	24223
Npc1	Niemann-Pick disease, type C1	266732
Ngfr	Nerve growth factor receptor	24596
Ifi47	Interferon gamma inducible protein 47	246208

doi:10.1371/journal.pone.0101835.t001

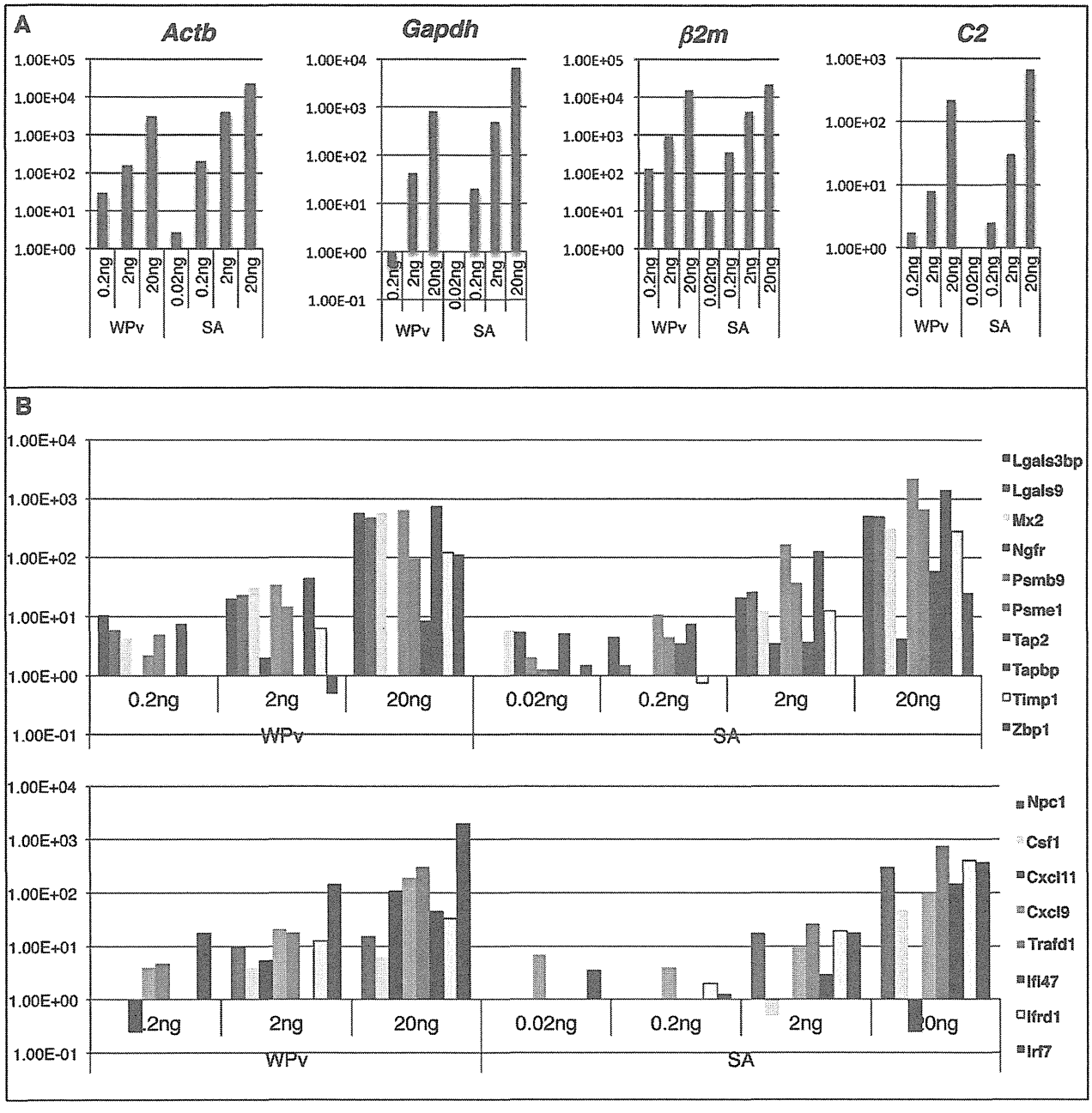

Figure 1. Optimization of QGP in influenza vaccine safety evaluation. A) Gene expression of *Actb*, *Gapdh*, *B2m* and *C2* and B) biomarkers, in 0.2, 2 and 20 ng RNA-containing samples from SA- and WPv-treated rat lungs. Relative expression levels of the *Gapdh* gene are indicated. SA: saline, WPv: Whole particle virion influenza vaccine.
doi:10.1371/journal.pone.0101835.g001

ers [HAv (Lot L03A) from Kaketsuken (Kumamoto), HAv (Lot 309) from Kitasato Institute (Saitama), HAv (Lot 343-A) from Denka Seiken Co., Ltd. (Tokyo), HAv (Lot HA082D) from Biken (Kagawa)] in Japan. All vaccines complied with the MRBP in Japan. HAv used in this study was tested and authorized by NCL (National Control Laboratory) for distribution in Japan.

3. Abnormal toxicity test

ATT was performed according to the MRBP [http://www.nih.go.jp/niid/en/mrbp-e.html] using rats with a slight modification. Each 5 ml of vaccine was intra-peritoneally (*i.p.*) injected into rats. Five milliliters of saline (SA) (Otsuka normal saline; Otsuka Pharmaceutical Factory Inc., Naruto, Tokushima, Japan) was *i.p.* injected as a control. One day after the injection, rat body weight was measured and peripheral blood was collected. The number of white blood cells was counted with a hemocytometer (Nihon Kohden, Japan).

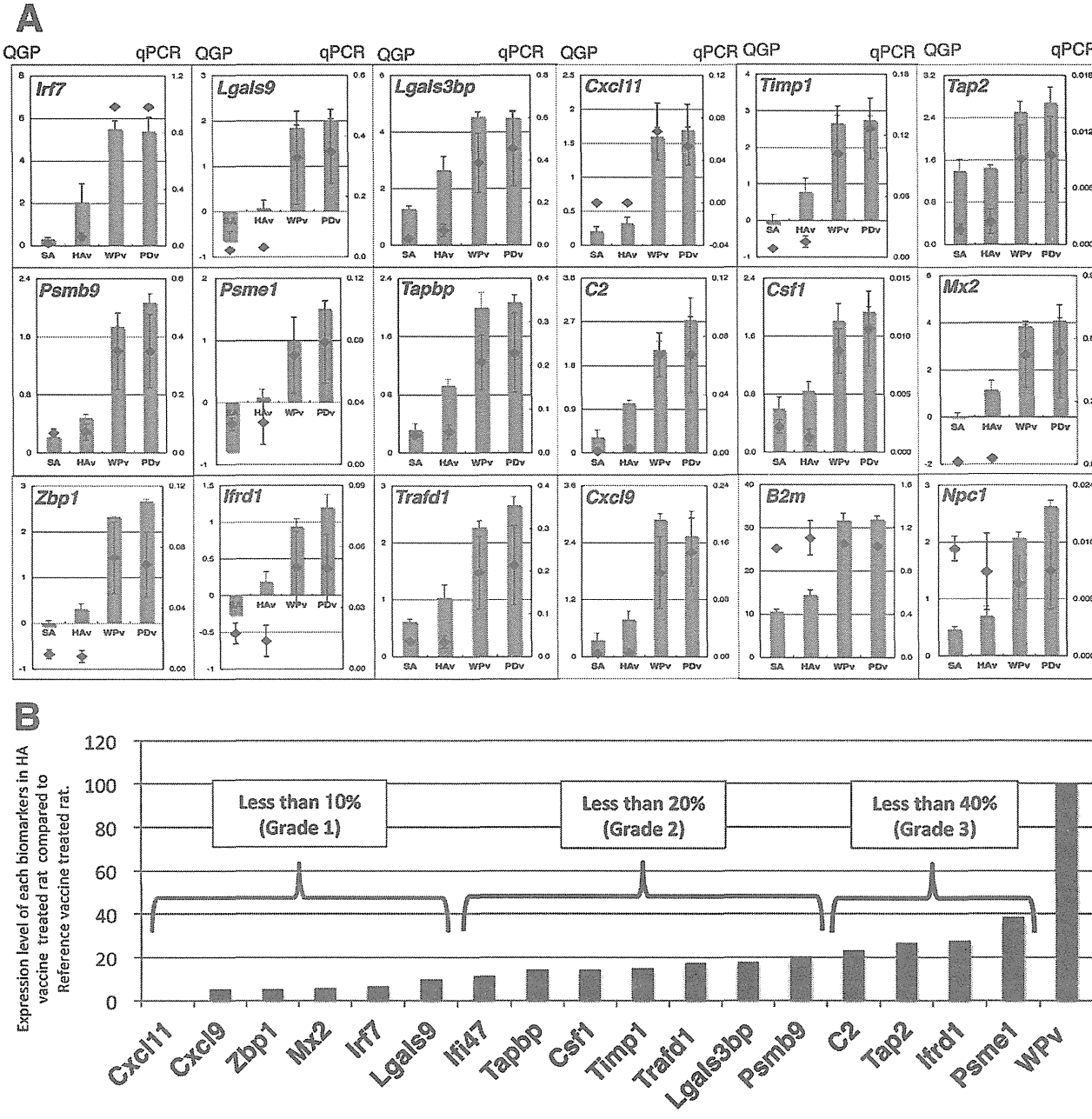

Figure 2. Validation of QGP with real-time PCR methods. A) GQP result was validated with real-time PCR methods. Bar graph indicates the real-time PCR results and dot blot indicates QGP results. B) Biomarkers were classified into three grades according to the relative expression level compared with WPv-treated rats.
doi:10.1371/journal.pone.0101835.g002

4. RNA preparation

One day after injection, rats were sacrificed to obtain whole lung tissues. Organs were immediately frozen in liquid nitrogen for storage. Thawed tissue was homogenized and mixed with an Isogen reagent (Nippon Gene, Tokyo, Japan). Total RNA was prepared from the lysate in accordance with the manufacturer's instructions. Poly (A)+ RNA was prepared from total RNA with a Poly (A) Purist Kit (Ambion, Austin, TX), according to the manufacturer's instructions.

5. Quantitative RT-PCR analysis

Poly (A)+ RNA was used to synthesize first-strand cDNA using a First-strand cDNA Synthesis Kit (Life Science Inc., St. Petersburg, FL), according to the manufacturer's instructions. Expression levels of biomarkers (**Table 1**) were analyzed by real-time polymerase chain reaction (PCR) using a 7500 Fast Real-Time PCR System (Applied Biosystems, Foster City, CA) with 7500 Fast System SDS Software Version 1.3. cDNA was amplified for real-time PCR using SYBR Green I (Molecular Probes Inc.) to detect the PCR products. One microliter of 6-fold diluted cDNA was

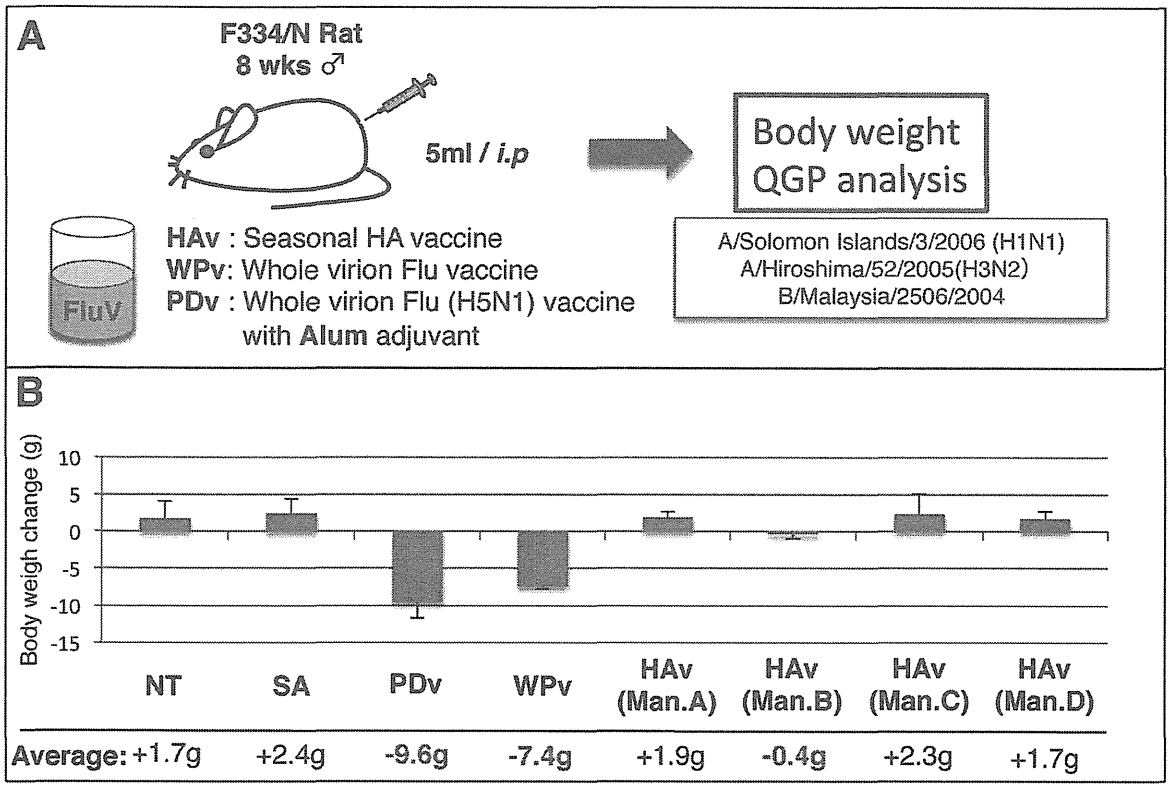

Figure 3. Evaluation of seasonal influenza vaccine with conventional animal safety test. A) The abnormal toxicity test was performed according to the Minimum Requirements of Biological Products. Each 5 ml vaccine was *i.p.* injected into rats, the body weight measured and lung tissues collected at day 1 after injection. B) Body weight change at day 1 after injection. NT: nontreated rat, SA: saline, PDv: pandemic H5N1 whole virion-derived vaccine with alum adjuvant, WPv: whole particle virion influenza vaccine, HAv: influenza HA vaccine, Man: manufacturer.
doi:10.1371/journal.pone.0101835.g003

used in a 20-μl final volume reaction containing 10 μl SYBR Green PCR Master Mix (Applied Biosystems), and forward and reverse primers were as described previously [13]. The 7500 Fast System was programmed to run an initial polymerase activation step at 95°C for 10 min followed by 40 cycles of denaturation (95°C for 15 s) and extension (60°C for 1 min). Product synthesis was monitored at the end of the extension step of each cycle. Gene expression values were normalized against rat GAPDH.

6. QuantiGene Plex assays

QuantiGene Plex (QGP) assays were performed according to the QuantiGene Plex Reagent System instructions (Panomics Inc., Fremont, CA), as described previously [11]. Briefly, 10 μl of starting poly (A)+RNA (50 ng) was incubated for 10 min at 65°C, then mixed with 33.3 μl of lysis mixture, 40 μl of capture buffer, 2 μl of capture beads, and 2 μl of the target gene-specific probe set. Probe sets were heated for 5 min prior to use. Each sample mixture was then dispensed into an individual well of a capture plate, sealed with foil tape and incubated at 54°C for 16–20 h. The hybridization mixture was transferred to a filter plate, and the wells were washed three times with 200 μl of wash buffer. Signals for the bound target mRNA were developed by sequential hybridization with branched DNA (bDNA) amplifier, and biotin-conjugated label probe, at 48°C for 1 h each. Two washes with wash buffer were used to remove unbound material after each hybridization step. Streptavidin-conjugated phycoerythrin was added to the wells and incubated at room temperature for 30 min. The luminescence of each well was measured using a Luminex 100 microtiter plate luminometer (Luminex). Two replicate assays measuring RNA directly (independent sampling n = 6 for mRNA, n = 3–5 for lysate) were performed for all described experiments. The 20 target genes and GAPDH mRNA were quantified, and the ratio of the target genes to GAPDH mRNA was calculated.

7. Statistical analysis

Multiple comparisons were performed for SA, PDv, WPv and HA. To determine differences between manufacturers, multiple comparisons were performed for SA and HA from manufacturers A, B, C and D. Statistical analysis was performed in GraphPad Prism 6 (GraphPad Software, La Jolla, CA) using an ordinary one-way analysis of variance test followed by a Tukey multiple comparison test.

Results

Optimization of multiple gene detection system, QuantiGene Plex, for safety evaluation of the influenza vaccine

We previously reported that 20 selected genes (**Table 1**), from 76 differentially expressed genes in adsorbed PDv-treated rats, could be used as biomarkers to evaluate H5N1 influenza vaccine safety compared with other types of influenza vaccine using conventional real-time PCR [13]. To establish faster and more convenient methods to detect these biomarkers in one-step as a new vaccine safety test, we used QuantiGene Plex (QGP)

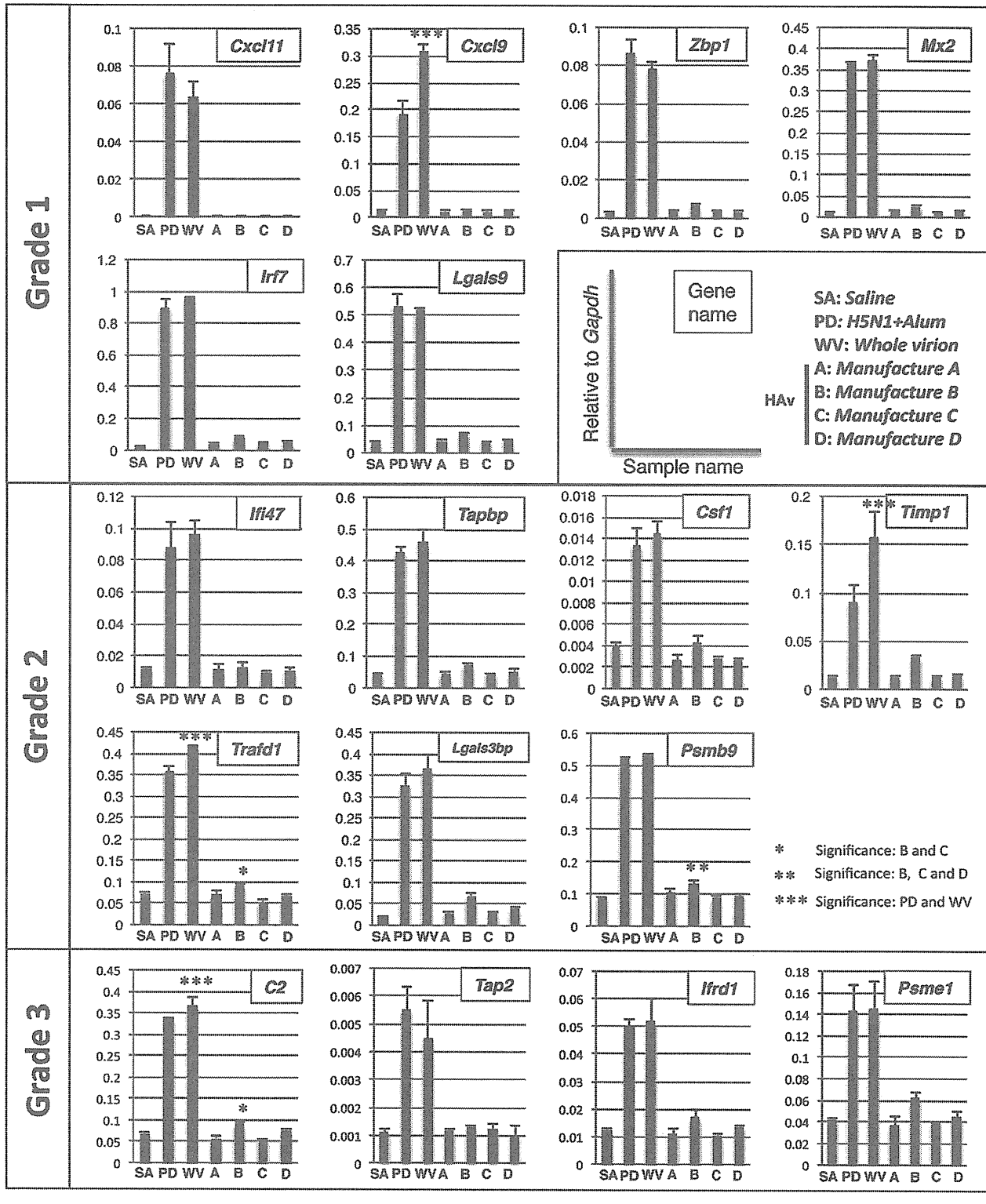

Figure 4. Evaluation of seasonal influenza vaccine with QGP. The relative gene expression levels of the *Gapdh* gene are indicated in each column (grades 1, 2 and 3, respectively). *Significant difference between B and C. **Significant difference between B, C and D, ***Significant difference between PD and WPv.
doi:10.1371/journal.pone.0101835.g004

technology (Panomics Inc., Fremont, CA). We designed a custom QGP 2.0 assay to enable the measurement of expression levels of identified biomarkers. The Panomics QGP 2.0 assays provided quantitative measurements of 3 to 80 target RNAs per well by

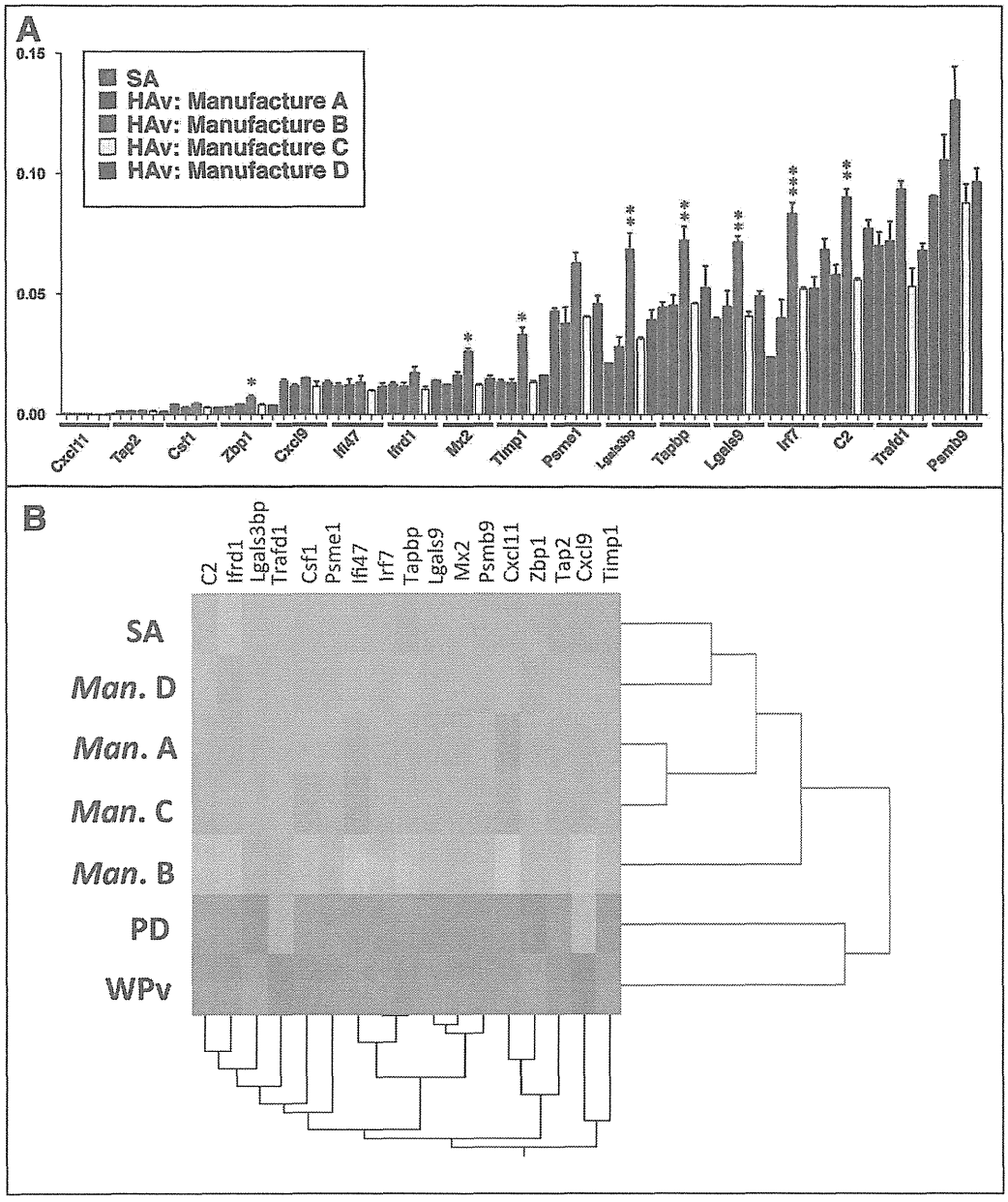

Figure 5. Evaluation of seasonal influenza vaccine with QGP and cluster analysis. A) Relative gene expression in HAv-treated rat lungs to *Gapdh* is indicated in the bar graph. B) Hierarchical clustering analysis with biomarkers could predict differences in HAv manufacturers as B is located in a separate cluster from other HAvs.
doi:10.1371/journal.pone.0101835.g005

using bDNA technology in conjunction with multi-analyte magnetic beads to provide the detection and quantitation of multiple mRNA targets simultaneously. bDNA technology is a hybridization-based methodology that uses labeled DNA probes to amplify the signal rather than the target mRNA. Here, we produced probes for 20 genes and two control genes (*Actb* and *Gapdh*) for the one-step detection and quantification of these biomarkers. To check the sensitivity of probes and dynamic range of our biomarkers, we prepared 0.02, 0.2, 2 and 20 ng total RNA samples from WPv and SA-treated rat lungs and performed QGP analysis. Two control genes and two biomarkers (*β2m* and *C2*) reacted in a dose-dependent manner (**Figure 1A**). We re-evaluated all probes with the same sample. Each biomarker reacted in a dose-dependent manner (**Figure 1B**) except *Ngfr* and *Npc1*. Therefore, 20 ng of RNA sample was used for multiplex gene detection. All biomarkers except *β2m* reacted in a dose-dependent manner. *β2m* was saturated when using 20 ng RNA sample; thus *β2m* could not be used for QGP analysis.

Validation of QGP with real-time PCR

To validate QGP, we performed real-time PCR analysis using the same samples. As a result, most biomarker gene expression data from the QGP correlated with the real-time PCR result except for *β2m*, *Npc1* (Figure 2) and *Ngfr* (data not shown). Finally,

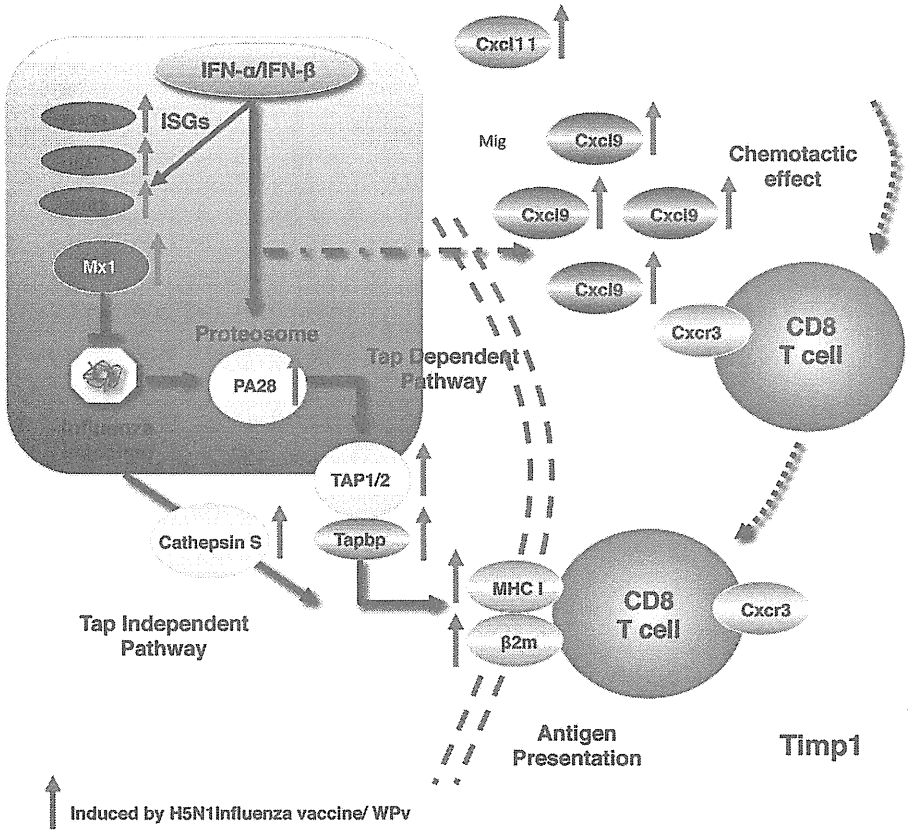

Figure 6. Summary of biomarker studies. Biomarkers used in this study were strongly correlated with immune responses after influenza infection.
doi:10.1371/journal.pone.0101835.g006

17 genes were selected as the multiplex detection biomarker set. We next determined the relative biomarker expression levels in HAv-treated rat lungs compared with WPv used as a reference toxicity vaccine in the leukopenic toxicity test (LTT) in Japan. We classified *Cxcl11*, *Cxcl9*, *Zbp1*, *Mx2*, *Irf7* and *Lgals9* as a "Grade 1" gene set where relative expression levels in HAv compared with WPv were less than 10%. Likewise, we classified *Ifi47*, *Tapbp*, *Csf1*, *Timp1*, *Trafd1*, *Lgals3bp* and *Psmb9* as a "Grade 2" gene set where relative expression levels were less than 20% and *C2*, *Tap2*, *Ifrd1* and *Psme1* as a "Grade 3" gene set where relative expression levels were less than 40% in HAv compared with WPv. In Japan, it is acceptable for leukopenic toxicity levels of HAv to be not more than 20% of WPv by LTT. We applied LTT criteria for selecting and subdividing these biomarkers into three grades with expression levels below 20% of WPv and others.

Evaluation of HAv safety in Japan using ATT and QGP

To evaluate the toxicity of seasonal HAv using biomarkers, we purchased market authorized seasonal influenza vaccines distributed in Japan from four different manufacturers (Kaketsuken, Denka Seiken, Kitasato, and Biken). Although the vaccines have been evaluated and passed ATT by the NCL according to the Japanese guidelines for MRBP, the reactogenicity of the vaccine to animals (rats, mice and guinea pigs) was varied. To evaluate these differences, we performed ATT and checked the body weight changes of rats after *i.p.* injection of each HAv (Figure 3A). Although treatment with PDv or WPv (toxic reference whole virion-derived vaccines) significantly decreased the body weight of rats, HAvs from three different manufacturers had no effect on body weight. HAv from manufacture B reduced the body weight of rats at day 1 (Figure 3B). However, there was no significant difference in rat body weight change for the other HAvs; thus HAv from manufacturer B might be slightly different, when comparing the mean body weight at day 1. In addition, there was no significant difference in leukocyte numbers following administration of HAv from the four manufacturers (data not shown). To evaluate the differences of each HAv, we next performed multiplex biomarker detection by QGP. No biomarkers were significantly up-regulated in HAv-treated rats compared with controls (Figure 4) except for *Psmb9*. Furthermore, *Psmb9* expression was significantly up-regulated following administration of HAv from manufacturer B compared with the control SA-treated and HAvs from the other manufacturers. The expression levels of *C2* and *Trafd1* were also significantly up-regulated in the HAv from manufacturer B compared with the HAv from manufacturer C.

Biomarkers to evaluate safety of adjuvanted influenza vaccine

Both PDv and WPv contain the whole virion influenza vaccine and alum adjuvant is only added to PDv to enhance its immunogenicity. There was no difference in body weight change between WPv- and PDv-treated rats (Figure 3B). However, among the 17 biomarkers, the expression level of three genes, *Cxcl9*, *Timp1* and *Trafd1* in PDv-treated rats were significantly decreased compared with WPv-treated rats (Figure 4). Thus, these biomarkers could potentially evaluate the aluminum adjuvant effect.

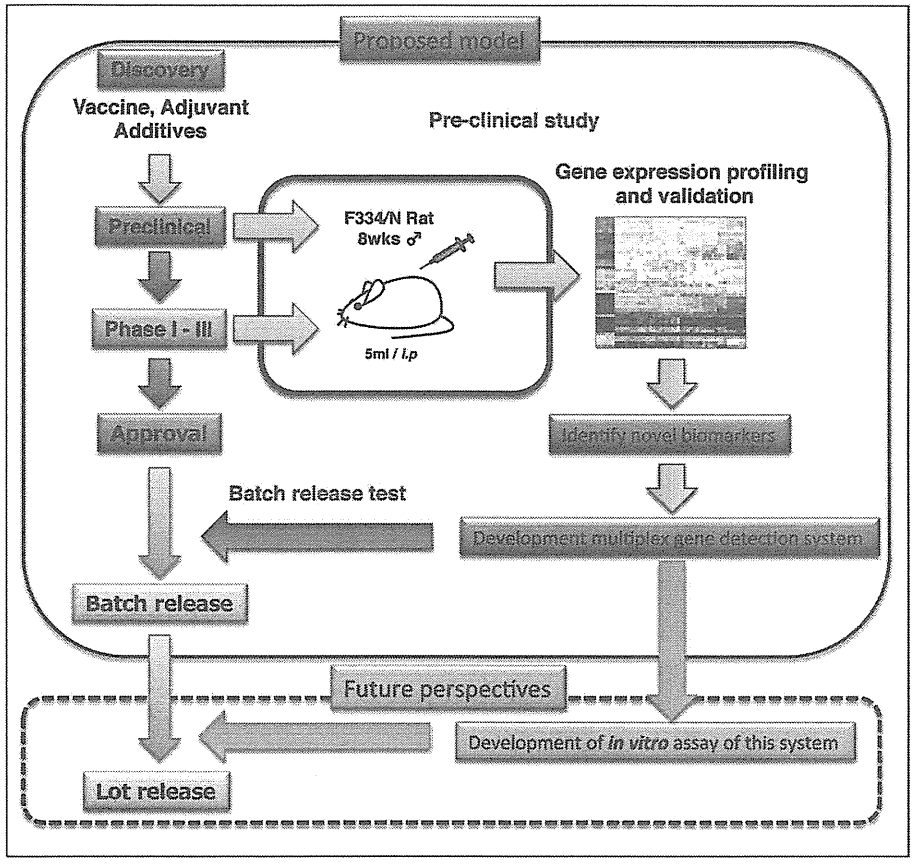

Figure 7. Application of the system biological approach for influenza vaccine development. Proposed model of future influenza vaccine development and establishment of preclinical studies and batch release testing. Acquisition of transcriptome data at the preclinical and clinical phase is useful for future batch release testing and the prediction of vaccine efficacy and toxicity.
doi:10.1371/journal.pone.0101835.g007

Cluster analysis of QGP data predicts influenza vaccine safety

Conventional animal tests such as ATT and LTT have been performed in Japan for the evaluation of influenza vaccine safety and toxicity. Despite applying these tests that evaluate whole virion-derived influenza vaccine from HAv, it is difficult to distinguish statistically between different HAvs if they do not have comparable toxicity greater than 20–50% to WPv. According to the body weight change observed with ATT, we speculated that HAv from manufacturer B was slightly different than the others tested (Figure 3B), although this was not statistically significant. However, when biomarkers were used with QGP to evaluate HAvs, we could distinguish the HAv from manufacturer B compared with those from other manufacturers. When we focused on biomarker expression among the HAv-treated rat lungs, the expression levels of *Zbp1*, *MX2*, *Timp1*, *Lgals3bp*, *Tapbp*, *Lgals9*, *Irf7* and *C2* were significantly up-regulated in rat lungs treated with HAvs from manufacturer B (Figure 5A). In addition, cluster analysis with the biomarkers predicted differences in HAvs as the vaccine from manufacturer B was located in a separate cluster from the other HAvs. Thus, these biomarkers can evaluate batch-to-batch and manufacturer-to-manufacturer differences in HAvs (Figure 5B).

Discussion

Vaccine safety is critical in the process of vaccine development and universal vaccination. Several vaccines were stopped owing to safety concerns, including severe side effects, after they had received marketing authorization and licensing, even when they were effective [14]. To ensure the safety of vaccines, the preclinical phase in the development of vaccines and the batch release system after marketing authorization is critical. However, the guidelines for nonclinical assessment of vaccines and batch release tests only focus on the evaluation of vaccine efficacy and immunogenicity in animal models, quality control testing programs and toxicology testing in relevant animal models [15]. These guidelines do not include scientific research for identifying the potential toxicities of the vaccines, adjuvants and additives.

We have demonstrated the advantage of a system biological approach using several vaccines authorized in Japan, *e.g.* DPT, JEV and Influenza vaccine including H5N1 pandemic influenza vaccine [10–13]. We successfully identified several biomarkers to evaluate DPT, JEV and influenza vaccine toxicity. In this study, we demonstrate that the biomarkers used to evaluate H5N1 pandemic influenza vaccine could also be used to evaluate the batch-to-batch consistency and the safety of HAvs. In addition, they can be used to evaluate manufacturer-to-manufacturer differences using the multiplex gene detection system. The biomarker analysis correlated to findings from conventional

animal use tests, such as ATT. In addition, sensitivity of toxicity detection and differences in HAvs was higher and more accurate than with conventional methods. Despite all the HAvs evaluated in this study meeting MRBP criteria and passing NCL, our results suggest that HAv from manufacturer B is slightly different than the HAvs according to *Lgals3bp*, *Tapbp*, *Lgals9*, *Irf7* and *C2* gene expression. Among the official vaccine adverse event information provided by the Japanese authorities, there is no reported evidence that the adverse event rate was increased or that severe adverse events were observed caused by HAv from manufacturer B. It is still unknown what factors (additives, formalin content, protein content) induce these biomarkers in the HAv from manufacturer B. Further studies are needed to determine whether our biomarkers could predict the toxicity of influenza vaccine by using different formulations of HAv. Using biomarkers from any grade characterized in this study, we could also predict the safety of influenza vaccines within 2 days whereas the conventional animal use safety test, ATT requires 7 days for evaluating batch-to-batch consistency and vaccine safety. Further studies are needed to determine how these biomarkers can be used to evaluate the safety of HAv. To set the percent limit of up-regulation of each biomarker, it might be helpful to compare another conventional test such as LTT [[http://www.nih.go.jp/niid/en/mrbp-e.html]] as well as a comparison of failed batches of HAv. LTT evaluates the peripheral leukocyte number reduction rate compared with WPv. In general, WPv induces a strong loss of peripheral leukocyte numbers 16 hours after WPv administration in mice [9 and 28]. The test criteria of LTT is that the loss of leukocyte numbers in test samples must be no greater than 20% compared with a reference toxic vaccine such as WPv or less than 50% of SA-treated mice. These criteria may be applicable to set our biomarker expression limit. Further validation is required to set the limit the gene expression level.

Influenza is a socially important infectious disease that causes seasonal flu outbreaks worldwide and has a pandemic status [16]. Correspondingly, many types of influenza vaccine (cell derived, recombinant derived, live attenuated and inactivated influenza vaccine), have been developed to ensure efficacy and reduce toxicity [17]. While some adjuvants have been developed and used to amplify vaccine efficacy [8], the safety of adjuvants is still of concern. Recently, several adjuvants (squalene-based MF59 and AS03) developed and licensed for use only in pandemic influenza vaccines were under investigation for the occurrence of narcolepsy in vaccinated children in European countries [18]. Conventional safety tests could be used to evaluate the safety of these vaccines [19], but it is still difficult to predict the safety and toxicity of influenza vaccines, adjuvants and additives [20]. We demonstrated that usage of system biological approaches to evaluate safety might revolutionize vaccine testing methods [21]. Most of the previously identified biomarkers were up-regulated and correlated with influenza infection, interferon responses, antigen presentation and antibody production (Figure 6). In addition, we found that several biomarkers, *Cxcl9*, *Trafd1*, and *C2* were candidates for evaluating differences between alum-adjuvanted influenza vaccines and nonadjuvanted vaccines. Further studies, using several adjuvants, are needed to confirm the feasibility of these biomarkers in evaluating adjuvant safety.

In addition to whole transcriptome analysis of vaccinated animals, recent advances in genome research enabled the acquisition of whole transcriptional data from vaccinated individuals and identification of gene expression after immunization with vaccines to yellow fever, measles, tularemia and tuberculosis [22]. With a focus on the influenza vaccine, Bucasas et al. reported a 494 gene set, including biomarkers identified in our previous study (*MX1*, *IRF7*) that strongly correlated with antibody responses in humans [23]. Wei et al. reported gene expression differences between HAv and live attenuated influenza vaccine. They identified 265 differentially expressed genes, including our previously identified biomarkers, *IRF7*, *MX1*, *MX2*, *OAS1* and *ZBP1* [24].

Recently, Nakaya and Pulendran reported a system biological approach, termed systems vaccinology [25], which was used to predict immunogenicity and provide new mechanistic insights regarding influenza vaccination. They also reported several gene sets that predicted influenza vaccine immunogenicity, including our previously identified biomarkers, *MX1*, *MX2*, *OAS1* and *IRF7* [26]. More recently, Franco et al. reported 20 genes, including our biomarkers, *TAP2* and *OAS1*, which correlated with antibody responses, using integrative genomic analysis [27]. All these reports suggest that using animal models is still useful if biomarkers are up-regulated in vaccinated individuals and can reveal the role of biomarkers in immune responses and vaccination toxicity. Thus, in the preclinical and clinical phase, the acquisition of transcriptome data from both vaccinated individuals and animals, and a comparison of these data will be helpful for future vaccine development and batch release testing (Figure 7).

Taken together, system biological approaches to identify vaccine toxicity using whole genome transcriptome methods will improve vaccine development in preclinical and clinical phases if more data are generated from successfully vaccinated individuals and those with side effects. It is still unclear whether and how these factors determine immunogenicity and toxicity. Further studies are required to identify and reveal the mechanisms underlying vaccination in humans and in animal models, including nonhuman primates.

Acknowledgments

The authors acknowledge Dr. Shinya Watanabe, Junichi-Imai for technical support of the initial transcriptome analysis after influenza vaccination of rats. The authors wish to thank Dr. Hiroshi Yamada for his advice on performing toxicogenomic studies.

Author Contributions

Conceived and designed the experiments: TM. Performed the experiments: TM HM MK KT. Analyzed the data: TM HM KJI IH KY. Contributed reagents/materials/analysis tools: TM HM MK KT KA KF KJI. Wrote the paper: TM.

References

1. Plotkin SL, Plotkin SA (2012) A short history of vaccination. General aspects of vaccination. In: Plotkin SA, Orenstein WA, Offit PA, editors. 6th edition Vaccines. Philadelphia: Saunders Elsevier. 1–13.
2. Baylor NW, Marshall VB (2012) Regulation and testing of vaccines. In: Plotkin SA, Orenstein WA, Offit PA, editors. 6th edition Vaccines. Philadelphia: Saunders Elsevier. 1427–1446.
3. Kurokawa M, Murata R (1961) On the Toxicity of the Toxoid Preparation Responsible for the Kyoto Catastrophe in 1948. Jpn J Med Sci Biol 14: 249–256.
4. Wood JM, Williams MS (1998) History of inactivated influenza vaccines. In: Nicholson KG, Webster RG, Hay AJ, editors. Textbook of influenza. Oxford: Blackwell Science. 317–323.
5. Nicholson KG, Tyrrell DA, Harrison P, Potter CW, Jennings R, et al. (1979) Clinical studies of monovalent inactivated whole virus and subunit A/USSR/77 (H1N1) vaccine: Serological responses and clinical reactions. J Biol Stand 7: 123–136.
6. Wright PF, Thompson J, Vaughn WK, Folland DS, Sell SH, et al. (1977) Trials of influenza A/New Jersey/76 virus vaccine in normal children: an overview of age-related antigenicity and reactogenicity. J Infect Dis 136: S731–S741.

7. Couch RB, Keitel WA, Cate TR (1997) Improvement of inactivated influenza virus vaccines. J Infect Dis. 176 Suppl 1: S38–44.
8. Even-Or O, Samira S, Ellis R, Kedar E, Barenholz Y (2013) Adjuvanted influenza vaccines. Expert Rev Vaccines. 12: 1095–1108.
9. Mizukami T, Masumi A, Momose H, Kuramitsu M, Takizawa K, et al. (2009) An improved abnormal toxicity test by using reference vaccine-specific body weight curves and histopathological data for monitoring vaccine quality and safety in Japan. Biologicals. 37: 8–17.
10. Hamaguchi I, Imai J, Momose H, Kawamura M, Mizukami T, et al. (2007) Two vaccine toxicity-related genes Agp and Hpx could prove useful for pertussis vaccine safety control. Vaccine. 25: 3355–3364.
11. Hamaguchi I, Imai J, Momose H, Kawamura M, Mizukami T, et al. (2008) Application of quantitative gene expression analysis for pertussis vaccine safety control. Vaccine. 26: 4686–4696.
12. Momose H, Imai J, Hamaguchi I, Kawamura M, Mizukami T, et al. (2010) Induction of indistinguishable gene expression patterns in rats by Vero cell-derived and mouse brain-derived Japanese encephalitis vaccines. Jpn J Infect Dis. 63: 25–30.
13. Mizukami T, Imai J, Hamaguchi I, Kawamura M, Momose H, et al. (2008) Application of DNA microarray technology to influenza A/Vietnam/1194/2004 (H5N1) vaccine safety evaluation. Vaccine. 26: 2270–2283.
14. Offit PA, Stefano FD (2012) Vaccine safety. In: Plotkin SA, Orenstein WA, Offit PA, editors. 6th edition Vaccines. Philadelphia: Saunders Elsevier. 1464–1480.
15. Wolf JJ, Kaplanski CV, Lebron JA (2010) Nonclinical safety assessment of vaccines and adjuvants. Methods Mol Biol. 626: 29–40.
16. WHO (2013) Pandemic Influenza Risk Management, WHO Interim Guidance. Available: http://www.who.int/influenza/preparedness/pandemic/GIP_PandemicInfluenzaRiskManagementInterimGuidance_Jun2013.pdf. Accessed 2014 June 18.
17. Wong SS, Webby RJ (2013) Traditional and new influenza vaccines. Clin Microbiol Rev. 26: 476–492.
18. Ahmed SS, Schur PH, Macdonald NE, Steinman L (2014). Narcolepsy, 2009 A (H1N1) pandemic influenza, and pandemic influenza vaccinations: What is known and unknown about the neurological disorder, the role for autoimmunity, and vaccine adjuvants. J Autoimmun. 50: 1–11.
19. Brennan FR1, Dougan G (2005) Non-clinical safety evaluation of novel vaccines and adjuvants: new products, new strategies. Vaccine. 23: 3210–3222.
20. Verdier F, Morgan L (2001) Predictive value of pre-clinical work for vaccine safety assessment. Vaccine. 20 Suppl 1: S21–23.
21. Momose H, Mizukami T, Ochiai M, Hamaguchi I, Yamaguchi K (2010) A new method for the evaluation of vaccine safety based on comprehensive gene expression analysis. J Biomed Biotechnol. 2010: 361841.
22. Wang IM, Bett AJ, Cristescu R, Loboda A, ter Meulen J (2012) Transcriptional profiling of vaccine-induced immune responses in humans and non-human primates. Microb Biotechnol. 5: 177–187.
23. Bucasas KL, Franco LM, Shaw CA, Bray MS, Wells JM, et al. (2011) Early patterns of gene expression correlate with the humoral immune response to influenza vaccination in humans. J Infect Dis. 203: 921–929.
24. Zhu W, Higgs BW, Morehouse C, Streicher K, Ambrose CS, et al. (2010) A whole genome transcriptional analysis of the early immune response induced by live attenuated and inactivated influenza vaccines in young children. Vaccine. 28: 2865–2876.
25. Pulendran B, Li S, Nakaya HI (2010) Systems vaccinology. Immunity. 33: 516–529.
26. Nakaya HI, Wrammert J, Lee EK, Racioppi L, Marie-Kunze S, et al. (2011) Systems biology of vaccination for seasonal influenza in humans. Nat Immunol. 12: 786–795.
27. Franco LM, Bucasas KL, Wells JM, Niño D, Wang X, et al. (2013) Integrative genomic analysis of the human immune response to influenza vaccination. Elife. 2: e00299.
28. Ato M, Takahashi Y, Fujii H, Hashimoto S, Kaji T, et al. (2013) Influenza A whole virion vaccine induces a rapid reduction of peripheral blood leukocytes via interferon-α-dependent apoptosis. Vaccine. 31: 2184–2190.

PLOS | ONE

B-Cell-Intrinsic Hepatitis C Virus Expression Leads to B-Cell-Lymphomagenesis and Induction of NF-κB Signalling

Yuri Kasama[1], Takuo Mizukami[2], Hideki Kusunoki[2], Jan Peveling-Oberhag[3], Yasumasa Nishito[4], Makoto Ozawa[6,7], Michinori Kohara[5], Toshiaki Mizuochi[2], Kyoko Tsukiyama-Kohara[6,7]*

1 Department of Experimental Phylaxiology, Faculty of Life Sciences, Kumamoto University, Kumamoto-shi, Kumamoto, Japan, **2** Department of Research on Blood and Biological Products, National Institute of Infectious Diseases, Musashi-Murayama-shi, Tokyo, Japan, **3** Department of Internal Medicine, Goethe-University Hospital, Frankfurt, Germany, **4** Center for Microarray Analysis, Tokyo Metropolitan Institute of Medical Science, Kamikitazawa, Tokyo, Japan, **5** Department of Microbiology and Cell Biology, Tokyo Metropolitan Institute of Medical Science, Kamikitazawa, Tokyo, Japan, **6** Transboundary Animal Diseases Center, Joint Faculty of Veterinary Medicine, Kagoshima University, Kagoshima, Japan, **7** Laboratory of Animal Hygiene, Joint Faculty of Veterinary Medicine, Kagoshima University, Kagoshima, Japan

Abstract

Hepatitis C virus (HCV) infection leads to the development of hepatic diseases, as well as extrahepatic disorders such as B-cell non-Hodgkin's lymphoma (B-NHL). To reveal the molecular signalling pathways responsible for HCV-associated B-NHL development, we utilised transgenic (Tg) mice that express the full-length HCV genome specifically in B cells and develop non-Hodgkin type B-cell lymphomas (BCLs). The gene expression profiles in B cells from BCL-developing HCV-Tg mice, from BCL-non-developing HCV-Tg mice, and from BCL-non-developing HCV-negative mice were analysed by genome-wide microarray. In BCLs from HCV-Tg mice, the expression of various genes was modified, and for some genes, expression was influenced by the gender of the animals. Markedly modified genes such as Fos, C3, LTβR, A20, NF-κB and miR-26b in BCLs were further characterised using specific assays. We propose that activation of both canonical and alternative NF-κB signalling pathways and down-regulation of miR-26b contribute to the development of HCV-associated B-NHL.

Citation: Kasama Y, Mizukami T, Kusunoki H, Peveling-Oberhag J, Nishito Y, et al. (2014) B-Cell-Intrinsic Hepatitis C Virus Expression Leads to B-Cell-Lymphomagenesis and Induction of NF-κB Signalling. PLoS ONE 9(3): e91373. doi:10.1371/journal.pone.0091373

Editor: Ranjit Ray, Saint Louis University, United States of America

Received December 16, 2013; **Accepted** February 10, 2014; **Published** March 20, 2014

Funding: This work was supported by grants from the Ministry of Education, Culture, Sports, Science and Technology of Japan (23590547) and the Ministry of Health, Labour and Welfare of Japan (H21-011). The funders had no role in study design, data collection and analysis, decision to publish, or preparation of the manuscript.

Competing Interests: The authors have declared that no competing interests exist.

* E-mail: kkohara@vet.kagoshima-u.ac.jp

Introduction

Approximately 200 million people are currently infected with the hepatitis C virus (HCV) worldwide [1]. HCV has been the major etiological agent of post-transfusion hepatitis and has frequently caused liver cirrhosis and hepatocellular carcinoma in chronic hepatitis C (CHC) patients [2,3]. Hepatocytes are considered to be the primary and major site of HCV replication; however, extrahepatic manifestations are commonly seen in CHC patients. For example, mixed cryoglobulinemia (MC), a systemic immune complex-mediated disorder characterised by B cell proliferation with the risk of evolving into overt B-cell non-Hodgkin's lymphoma (B-NHL), is frequently recognised in CHC patients [4–6]. We have previously demonstrated the presence of both HCV RNA and viral proteins in peripheral B cells of CHC patients [7], although the mode of HCV infection and possible HCV replication in peripheral B cells remains a matter of debate. Furthermore, in the last two decades, an array of epidemiological evidence has accumulated involving the association between HCV infection and the occurrence of several hematologic malignancies, most notably B-NHL [8], [9]. The most compelling argument for a causal relationship between HCV and the occurrence of B-NHL is made by interventional studies demonstrating that a sustained virologic response to antiviral treatments, including the interferon α-induced regression of HCV-associated lymphomas and viral relapse after the initial virologic response, led to lymphoma recurrence [10]. However, the mechanisms underlying the cause-and-effect relationship are mostly unknown.

One of the potential host factors involved in HCV-associated B-NHL development is activator protein 1 (AP-1), which is primarily composed of c-Jun, c-Fos, and JunB, while JunD or Fra-1, Fra-2 and FosB are involved less frequently [11]. AP-1 is involved in B cell lymphomagenesis, is repressed by B cell lymphoma-6 [12] and is inhibited by the overexpression of T cell leukaemia/lymphoma 1, which resulted in the enhancement of nuclear factor kappa B (NF-κB) [13].

NF-κB is a ubiquitously expressed transcription factor that regulates a wide array of cellular processes, including the immune response, cell growth and differentiation [14,15]. The activation of NF-κB is regulated by two distinct pathways termed the 'canonical' and the 'alternative' NF-κB signalling pathways. Representative stimulators of the canonical and alternative pathways are tumour necrosis factor αTNFα) and lymphotoxin α and β (LTα and LTβ), respectively [16]. Previous studies have demonstrated that NF-κB is activated via both the canonical [17,18] and alternative [19] pathways in chronic HCV infection

[17,18] and HCV-related B-NHL [20]. However, the key NF-κB-activating pathway involved in HCV-associated B-NHL remains unknown.

TNFα-induced protein 3 (TNFAIP3), also known as A20, was first identified as a TNF-induced cytoplasmic protein with zinc finger motifs [21]. A20 has since been described as playing a pivotal role in the negative regulation of inflammation by terminating the canonical NF-κB signalling pathway [22–24]. Recently, A20 has gained attention as a novel tumour suppressor. For example, A20 was reported to be frequently inactivated or even deleted from mantle-cell lymphoma [25,26] and diffuse large B-cell lymphoma (DLBCL) [27]. These findings raise the possibility that inactivation of A20 is, at least partially, responsible for lymphomagenesis [28–30]. Other investigators have subsequently confirmed these findings [27,31]. Moreover, A20 also regulates antiviral signalling [32] as well as programmed cell death [33–35].

microRNAs (miRNAs) play a role in controlling various biological functions, including cell differentiation, growth regulation and transcriptional regulation [36]. In general, the dysfunctional expression of miRNAs is considered to be a common hallmark of cancers, including lymphomas [37]. HCV has been shown to influence miRNA expression *in vivo* and *in vitro* and utilises the liver-specific microRNA miR-122 for its replication [38]. The expression of miRNAs is also known to involve NF-κB activation. For example, miR-125a and miR-125b, both of which are often duplicated and/or overexpressed in DLBCL, were shown to activate NF-κB by targeting the A20 [39] and NF-κB-mediated dysregulation of miRNAs observed in lymphoma[40]. Moreover, global miRNA expression profiling analysis revealed miR-26b down-regulation in HCV-related splenic marginal zone lymphomas (SMZL) [41]. The same miRNA was found to be downregulated in peripheral blood mononuclear cells (PBMCs) from HCV-positive MC and NHL subjects [42].

We recently established transgenic mice that express the full-length HCV genome specifically in B cells (HCV-Tg mice) and observed the incidence of non-Hodgkin type B-cell lymphoma (BCL), primarily DLBCL, within 600 days after birth in approximately 25% of the HCV-Tg mice [43]. This experimental model is a useful tool for analysing the mechanisms underlying the development of HCV-associated manifestations such as B-NHL. To reveal the molecular signalling pathways responsible for HCV-associated B-NHL development, we performed a comprehensive molecular analysis of BCLs in HCV-Tg mice using a genome-wide microarray. We also characterised miR-26b expression in BCLs from HCV-Tg mice. Our results suggest that the activation of both canonical and alternative NF-κB pathways is involved in HCV-associated B-NHL development.

Materials and Methods

Ethics Statement

This study was carried out in strict accordance with both the Guidelines for Animal Experimentation of the Japanese Association for Laboratory Animal Science and the Guide for the Care and Use of Laboratory Animals of the National Institutes of Health. All experiment protocols were approved by the institutional review boards of the regional ethics committees of Kumamoto University (A22-136) and Kagoshima University (H24-008).

Animal experiments

The full-length HCV genome (Rz) under the conditional Cre/*lox*P expression system [44] with mice expressing the Cre enzyme under the transcriptional control of the B lineage–restricted gene *CD19* [45] was established as RzCD19Cre mice [43]. Wild-type (WT), Rz, CD19Cre, RzCD19Cre mice (129/sv, BALB/c and C57BL/6J mixed background) were maintained in conventional animal housing under specific pathogen-free conditions. CD19Cre and RzCD19Cre mice were bred to be heterozygous for the *Cre* allele.

Isolation of B cells and their RNAs

Mouse B cells were isolated using MACS^{R} beads (Milteny Biotec, Bergisch Gladbach, Germany) and anti-CD19 antibody (Beckton Dickinson, Franklin Lake, NJ). For FACS analysis, B and T cell populations were characterised using FITC-conjugated anti-B220 antibody (Milteny Biotec) and phycoerythrin (PE)-conjugated anti-CD3 antibody (Milteny Biotec) (Figure S1A). B cell purity was routinely over 95%. Total RNA was extracted from the B cells using the acid guanidine thiocyanate phenol chloroform method [44,46]. The RNA integrity number was measured with an Agilent 2100 Bioanalyzer (Agilent Technologies, Santa Clara, CA), and samples with values over 8.0 were subjected to microarray analysis (Figure S1B).

Microarray analysis

For microarray analysis, total RNAs were extracted, and RNA integrity was assessed using a Bioanalyzer (Agilent Technologies). cRNA targets were synthesised and hybridised with Whole Mouse Genome Microarray (G4846A; Agilent Technologies), in accordance with the manufacturer's instructions. More than 2-fold changes in gene expression were considered to be significant. Array data were analysed using MetaCore^{TM} software (Thomson Reuters Co., New York, NY). The results of microarray analysis

Table 1. Mice subjected to microarray analysis.

Pairing	Mouse genotype	Mouse (No)	Age (d)	Sex	Remarks
1	RzCD19Cre	24–1	748	male	HCV(+)BCL*
		59–1	723	male	
		69–5	710	male	
	RzCD19Cre	248–1	860	male	HCV(+) B cell
		288–3	472	male	
		299–1	385	male	
2	RzCD19Cre	307–2	212	male	HCV(+) B cell
		307–3	212	male	
	Rz, 4EBP(+/−)+	307–1	220	male	HCV(−) B cell
		312–1	220	male	
3	RzCD19Cre	54–1	724	female	HCV(+)BCL
		62–2	723	female	
	RzCD19Cre	308–4	219	female	HCV(+) B cell
		308–6	219	female	
4	RzCD19Cre	308–4	219	female	HCV(+) B cell
		308–6	219	female	
	Rz	308–1	219	female	HCV(−) B cell
		308–3	219	female	

*BCL: B cell lymphoma; +4EBP(+/−): heterozygous knockout of 4E-BP1 gene [73].

doi:10.1371/journal.pone.0091373.t001

A Disease network

Pairing 1 (HCV+B vs HCV+BCL, male)

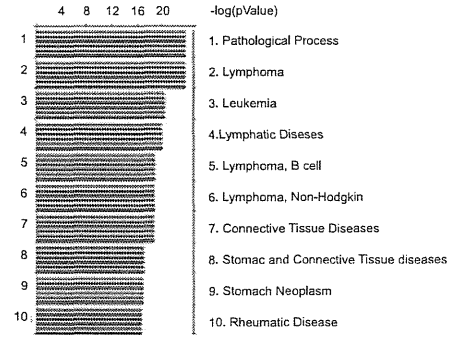

Pairing 2 (HCV+ vs HCV-, B cells, male)

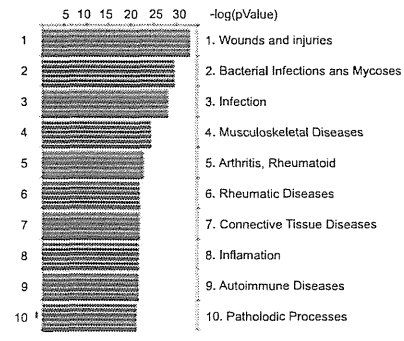

Pairing 3 (HCV+B vs HCV+BCL, female)

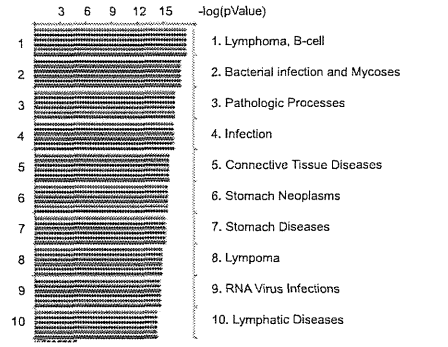

Pairing 4 (HCV+ vs HCV-, B cells, female)

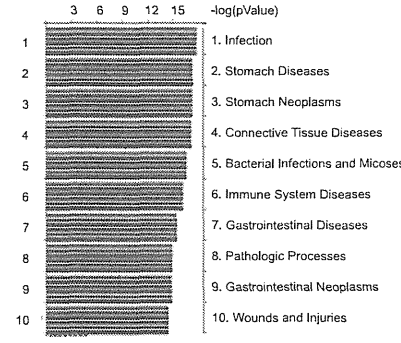

B Process network

Pairing 1 (HCV+B vs HCV+BCL, male)

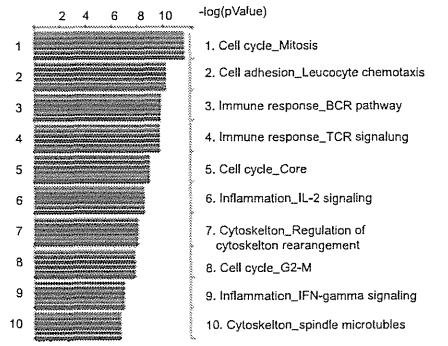

Pairing 2 (HCV+ vs HCV-, B cells, male)

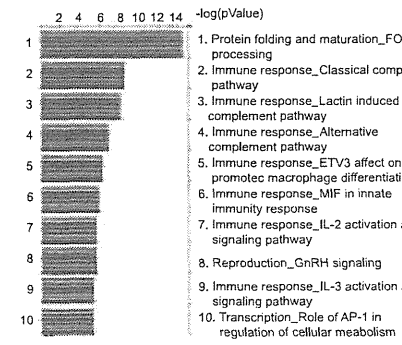

Pairing 3 (HCV+B vs HCV+BCL, female)

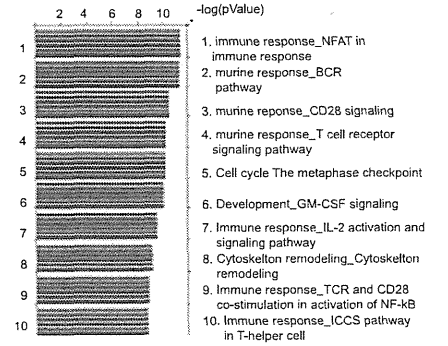

Pairing 4 (HCV+ vs HCV-, B cells, female)

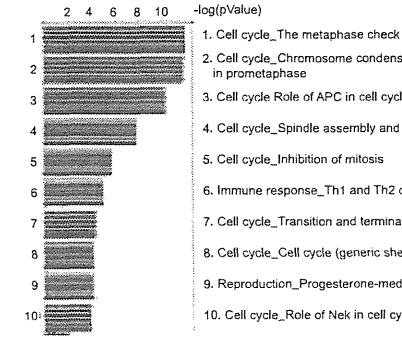

Figure 1. Data from array performed once with mixed RNA samples (Table 1) were analysed using MetaCore software. Signals were analysed in the disease network (**A**) and in the process network (**B**) the values for the microarray data [(Feature number; yellow), (Process Signal (635); blue), (Process signal (532); red), Test/Control (532/635); green], (Process Signal (635); orange), (Process signal (532); purple)] are indicated by coloured bars. Abbreviations: BCL = B cell lymphoma. Refer to Table 1 for construction of pairings.
doi:10.1371/journal.pone.0091373.g001

were registered in the Gene Expression Omnibus (GEO) database under the accession number GSE54722.

Quantitative RT-PCR

cDNA was synthesised from 0.5 or 1 μg of total RNA with a Superscript II kit (Life Technologies, Carlsbad, CA). TaqMan gene expression assays were custom-designed and manufactured by Life Technologies. RNA expression was quantified using the ABI 7500 real-time PCR system (Life Technologies) or the CFX96 system (BioRad, Hercules, CA).

Western blot analysis

Whole-cell proteins were extracted using RIPA buffer. Protein concentrations were determined using the BCA Protein assay Kit-Reducing Agent Compatible (Pierce Biotechnology, Rockford, IL). Samples (~10 μg) were loaded onto 10% SDS acrylamide gels, and gels were then transferred to PVDF membranes (Merck Millipore, Darmstadt, Germany). Membranes were blocked using 5% (w/v) non-fat milk for approximately 1 hour at room temperature and were then sequentially probed with primary and secondary antibodies at 4°C overnight and at room temperature for approximately 1 hour, respectively.

As primary antibodies, anti-A20 antibody (sc-166692; Santa Cruz Biotech, Dallas, TX), anti-A20 antibody (SAB3500036; Sigma-Aldrich, St. Louis, MO), anti-C3 antibody (D-19; Santa Cruz Biotech), anti-Fos (sc-52; Santa Cruz Biotech), anti-c-Jun(N) (sc-45; Santa Cruz Biotech) and anti-GAPDH-HRP (sc-20357; Santa Cruz Biotech) antibodies were used. Secondary antibodies used were horseradish peroxidase-coupled donkey anti-rabbit Ig (NA934; GE Healthcare, Buckinghamshire, UK) and horseradish peroxidase-coupled sheep anti-mouse Ig (NA931; GE Healthcare). Protein bands were detected and quantified using either Super-Signal West Dura or Femto Extended Duration Substrate (Pierce Biotechnology) with a LAS-3000 Image Analyzer (Fuji Film, Tokyo, Japan). Stripping and re-probing of the Western blots were performed using Re-blot plus mild antibody stripping solution (Merck Millipore).

Histological preparation

Liver, spleen, thymus and lymph nodes were harvested from HCV-Tg mice and fixed in 4% (wt/vol) paraformaldehyde in phosphate-buffered saline (pH 7.5) at 4°C for 24 hours. After fixation, samples were dehydrated in a graded ethanol series, cleared in xylene and embedded in paraffin, and 4-μm semi-thin sections were prepared using a carbon steel blade (Feather Safety Razor Co., Osaka, Japan) on a microtome (Yamato Kouki, Tokyo, Japan). Tissue sections were mounted on super-frosted glass slides coated with methyl-amino-silane (Matsunami Glass, Osaka, Japan). Histological images were acquired using an Olympus BX53 microscope (Olympus, Tokyo, Japan) equipped with 10×/0.30, 20×/0.50, 40×/0.75, and 100×/1.30 NA objective lenses. Images were captured using an Olympus DP73 (Olympus) under an Olympus FV1000 confocal microscope (Olympus).

Immunofluorescence

Anti-mouse NF-κB p65 antibody (Ab7970; Abcam, Cambridge, UK) and anti-mouse B220 (14-0452-81; eBioscience, San Diego, CA) were used as primary antibodies, and donkey anti-rat IgG-Alexa Fluor 488 [712-545-153; Jackson ImmunoResearch Laboratories Inc. (JIR), West Grove, PA], donkey anti-rabbit IgG-Alexa Fluor 488 (711-545-152; JIR), donkey anti-rat IgG-Cy3 (712-165-153; JIR) and donkey anti-rabbit IgG-Cy3 (711-165-152; JIR) were used as secondary antibodies. Staining was conducted as described previously [47]. Briefly, antigen retrieval was performed in a steam pressure cooker with prewarmed antigen retrieval buffer, citrate pH 6 (S203130; Dako, Glostrup, Denmark) at 95°C for 15 min. After blocking with 3% bovine serum albumin in phosphate-buffered saline, sections (4 μm) were incubated with anti-NF-κB, -Iκ-B, -B200 or -A20 antibodies at a 1:200 dilution each at 4°C overnight. Sections were incubated with secondary antibodies and anti-rat Alexa Fluor 488, -rabbit Alexa Fluor 488, -rat Alexa Fluor 546, and -rabbit Alexa Fluor 546 at room temperature for 2 hours. Nuclei were stained with Hoechst 333421 (H3570; Life Technologies).

Single assay stem-loop Q-RT-PCR/ miR-26b analysis

Formalin-fixed, paraffin-embedded (FFPE) splenic tissue from 24 animals (BCL HCV+, n = 8; BCL HCV-, n = 5; non-tumorous spleen HCV+/−, n = 11) was selected for miR-26b expression analysis. Total RNA was extracted using an RNeasy FFPE Kit (Qiagen, Hilden, Germany) in accordance with the manufacturer's protocol. Single assay stem-loop Q-RT-PCR (TaqMan MicroRNA assays, Life Technologies) was used to quantify miRNAs in accordance with the manufacturer's protocol. Total RNA input for each reaction was 50 ng. Expression was analysed for hsa-miR-26b and an endogenous control (snoRNA202). Each sample was analysed in triplicate, and delta C_t values were calculated using endogenous controls.

Statistics

For statistical analysis of NF-κB localisation, approximately 30–100 cells were randomly selected from each section area (two sections were used), and the cells double-positive for NF-κB and B220 were counted. All statistical analyses were performed using Prism software, version 5 (GraphPad, San Diego, CA). All experiments were independently performed three times, and a two-tailed Student *t*-test was applied to verify whether the results were significantly changed compared to the control ($P<0.05$).

Results

Characterisation of gene expression in B cells from HCV-Tg mice by microarray analysis

We previously established HCV-Tg mice that develop spontaneous BCL with a high penetrance (approximately 25%) [43]. To clarify the mechanisms of the HCV-associated B-NHL development using this mouse model, we performed a comprehensive gene expression analysis using a genome-wide microarray. B cells were isolated from BCL-developing HCV-Tg mice (Table 1, upper columns of pairing 1 and 3), from BCL-non-developing HCV-Tg mice (lower columns of pairing 1 and 3 and upper columns of pairing 2 and 4), and from BCL-non-developing HCV-negative mice (lower columns of pairing 2 and 4). RNA was purified from these B cells (Figure S1) and was characterised by microarray analysis (data not shown). In B cells isolated from BCL-non-developing HCV-Tg male mice, 455 and 863 genes were up-

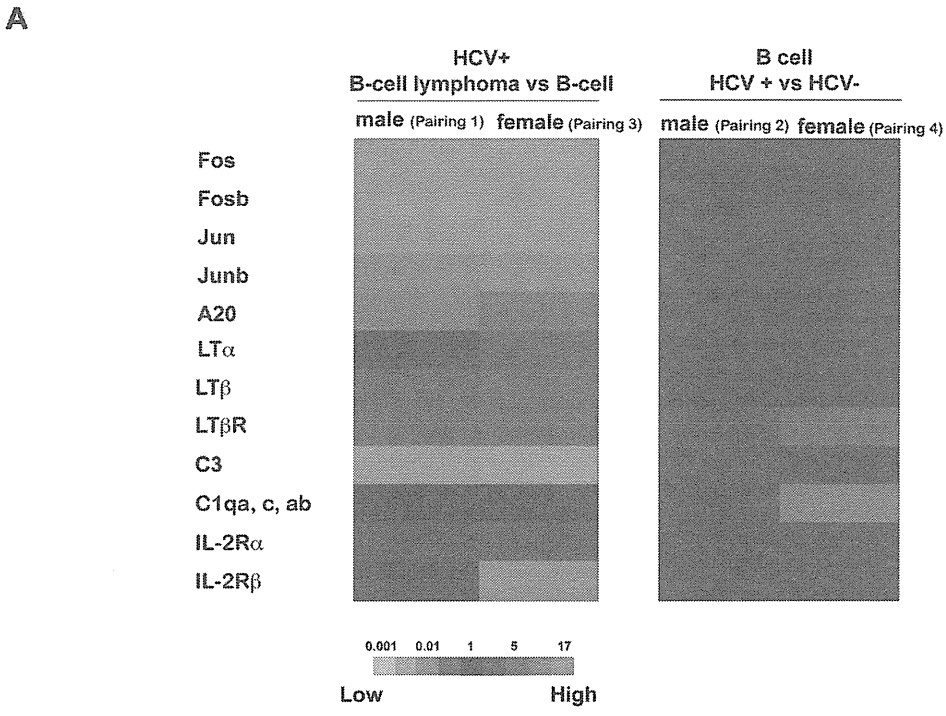
A
HCV+
B-cell lymphoma vs B-cell
B cell
HCV + vs HCV-
male (Pairing 1) female (Pairing 3)
male (Pairing 2) female (Pairing 4)
Fos
Fosb
Jun
Junb
A20
LTα
LTβ
LTβR
C3
C1qa, c, ab
IL-2Rα
IL-2Rβ
0.001 0.01 1 5 17
Low
High

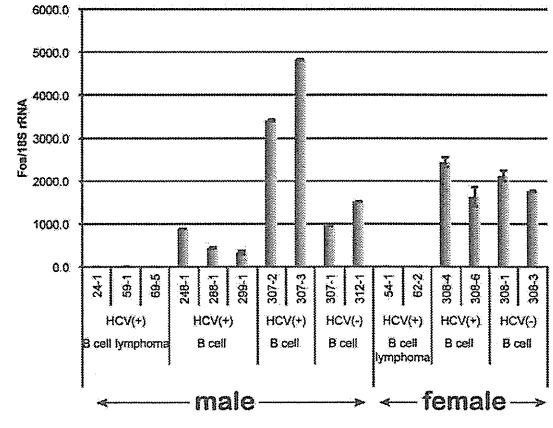
B
Fos/18S rRNA
6000.0
5000.0
4000.0
3000.0
2000.0
1000.0
0.0
24-1 59-1 69-5 248-1 288-1 299-1 307-2 307-3 307-1 312-1 54-1 62-2 308-4 308-6 308-1 308-3
HCV(+) B cell lymphoma
HCV(+) B cell
HCV(+) B cell
HCV(-) B cell
HCV(+) B cell lymphoma
HCV(+) B cell
HCV(-) B cell
male
female

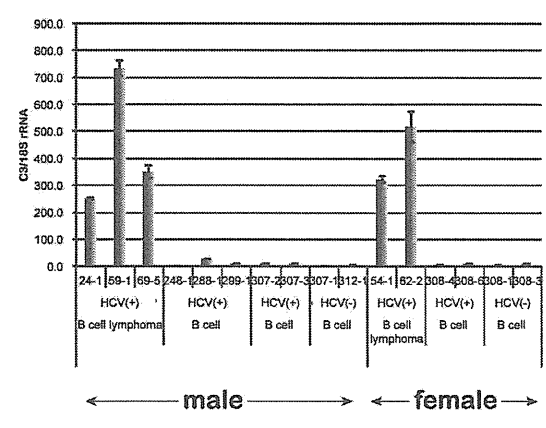
C
C3/18S rRNA
900.0
800.0
700.0
600.0
500.0
400.0
300.0
200.0
100.0
0.0
24-1 59-1 69-5 248-1 288-1 299-1 307-2 307-3 307-1 312-1 54-1 62-2 308-4 308-6 308-1 308-3
HCV(+) B cell lymphoma
HCV(+) B cell
HCV(+) B cell
HCV(-) B cell
HCV(+) B cell lymphoma
HCV(+) B cell
HCV(-) B cell
male
female

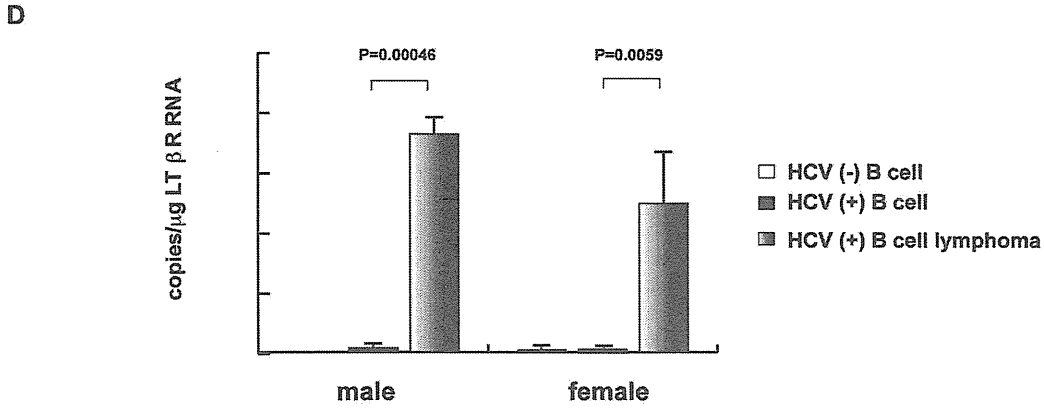
D
P=0.00046
P=0.0059
copies/μg LT β R RNA
male
female
HCV (-) B cell
HCV (+) B cell
HCV (+) B cell lymphoma

Figure 2. The expression of genes involved in oncogenic pathways associated with BCL. A: Highly modified gene signals in B cell lymphoma in RzCD19Cre mice BCL vs. B cells in RzCD19Cre male (Pair 1) or female (Pair 3) mice (left), and the genes modified by HCV expression in B cells in male (Pair 2) or female (Pair 4) (right). Red indicates the relative enhancement of the expression ratio of the processed signal (Test/Control, 532/635), and green indicates the relative reduction of expression. **B**: Quantification of Fos mRNA in HCV-, HCV+ B cells and HCV-Tg BCL in mice (numbers of individual mice were indicated) by quantitative RT-PCR. Fos mRNA was normalised against 18S rRNA, and the relative ratio was calculated. Vertical bars indicate S.D. **C**: Quantification of C3 mRNA in HCV-, HCV+ B cells and HCV-Tg BCL in mice. C3 mRNA was normalised against 18S rRNA, and relative ratio was calculated. Vertical bars indicate S.D. **D**: Quantification of LT βR mRNA in HCV-, HCV+ B cells and HCV-Tg BCL in mice by quantitative RT-PCR. RNA copies per total RNA (μg) were indicated and vertical bars indicate S.D.
doi:10.1371/journal.pone.0091373.g002

and down-regulated, respectively, compared with the HCV-negative counterparts (Table 1, pairing 2); whereas 133 and 331 genes were up- and down-regulated, respectively, in BCL-non-developing HCV-Tg female mice (Table 1, pairing 4). Furthermore, 1,682 and 2,383 genes were up- and down-regulated, respectively, in BCL-developing HCV-Tg male mice compared to their BCL-non-developing counterparts (Table 1, pairing 1); whereas 2,089 and 2,565 genes were up- and down-regulated, respectively, in BCL-developing HCV-Tg female mice (Table 1, pairing 3).

Metacore analysis of microarray results

In order to characterize the cellular processes affected by the gene expression changes, we carried out a pathway analysis of microarray data of pairings 1–4 (Table 1) using MetaCore™ software. This data mining revealed that lymphoma, leukaemia, B cell lymphoma, and lymphatic disease pathways were appreciably modified in pairings 1 and 3 with high frequency (Figure 1a). In pairings 2 and 4, the modifications involving wound healing and infection pathways were highlighted, respectively. In the process network, the cell cycle and immune response (B cell receptor, T cell receptor, and IL-2) pathways were greatly modified in pairings 1 and 3 (Figure 1b). The immune response (complement, macrophage, IL-2, and IL-3 in group 2; Th1 and Th2 in pairing), protein folding (in pairing 2), and cell cycle (in pairing 4) pathways were also modified.

Dysregulated genes in HCV-associated B-cell lymphoma

In addition to the pathways analysis, we also carefully examined the expression of genes involved in oncogenic pathways associated with BCL. Expression of Fos, Fosb, Jun and Junb was markedly down-regulated in BCL obtained from HCV-Tg mice (Figure 2a). Similarly, the expression of A20 and LTβ was greatly down-regulated in BCL (Figure 2a). In contrast, the expression of the LTβ receptor (LTβR), the IL-2 receptor α(IL-2Rα, IL-2Rβ and complement C3 was up-regulated in the examined BCLs (Figure 2a). While alterations in the gene expression of LTα and IL-2Rβ differed between males and females, the overall mRNA expression profile in the BCL analysed from HCV-Tg mice essentially showed no differences between male and female mice. In addition, clinically, there was no clear gender priority in HCV-NHL [48–50]. These results suggest that the molecular signalling pathways leading to HCV-associated B-NHL development are common to males and females.

In non-tumorous B cells from BCL-non-developing HCV-Tg male mice, the expression of LTβR and C3 was up-regulated when compared with HCV-negative counterparts (Figure 2a). In contrast, in female counterparts, the expression of LTβR and complements C1qa, c, and ab was down-regulated (Figure 2a, Pair. 4). These results suggest that the impact of HCV infection in B cells may be different between males and females.

Expression of Fos, C3, and LTβR genes in HCV-associated BCL

In order to validate the microarray results, levels of Fos and C3 mRNAs were quantified by real-time PCR. Striking down-regulation of Fos gene expression was observed in BCLs from HCV-Tg mice (Figure 2b). In contrast, C3 mRNA expression was markedly up-regulated in BCLs from HCV-Tg mice (Figure 2c). These results were consistent with the microarray data (Figure 2a, GEO accession number GSE54722). Similarly, the mRNA expression of the LTβR gene was significantly increased in HCV-associated BCLs (Figure 2d), confirming the microarray analysis results (Figure 2a). Importantly, these changes occurred in both male and female mice.

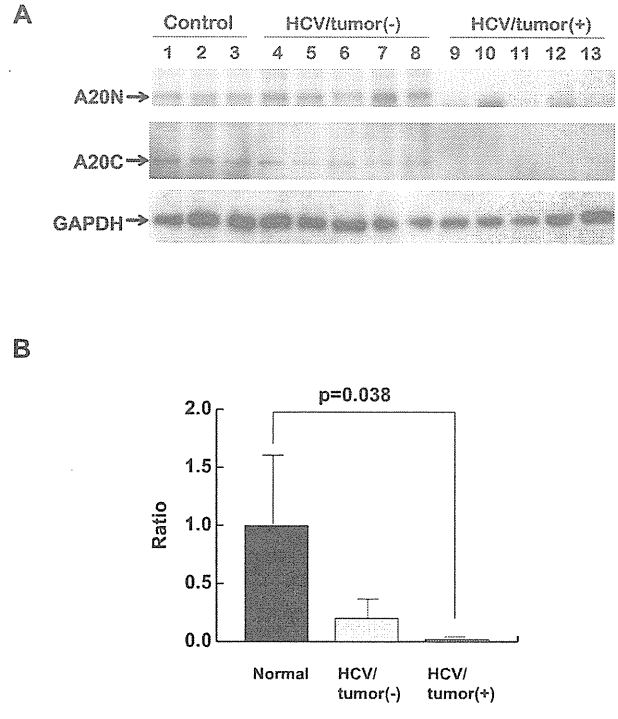

Figure 3. The expression of A20 in HCV-associated BCL. A: Expression levels of A20 in the spleen from RzCD19Cre mice with or without BCL. Whole-tissue extracts prepared from the spleen in CD19Cre mice (control, n = 3; lanes 1–3 217–2, 2 224–2, 224–3), RzCD19Cre mice without BCL (HCV/Tumour(-), n = 5; lanes 4–8 217–3, 224–4, 232–3, 254–4, 240–2) and RzCD19Cre mice with BCL (HCV/Tumour(+), n = 5; lanes 9–13 24–1, 56–5, 69–5, 59–1, 43–4) were subjected to SDS-PAGE and were analysed by immunoblotting using anti-N terminal (A20N), anti-C terminal A20 (A20C), and anti-GAPDH antibodies. GAPDH was used as protein loading control. **B**: Quantitation of A20 (N and C), the average is indicated and statistical analysis was performed. Vertical bars indicate S.D.
doi:10.1371/journal.pone.0091373.g003

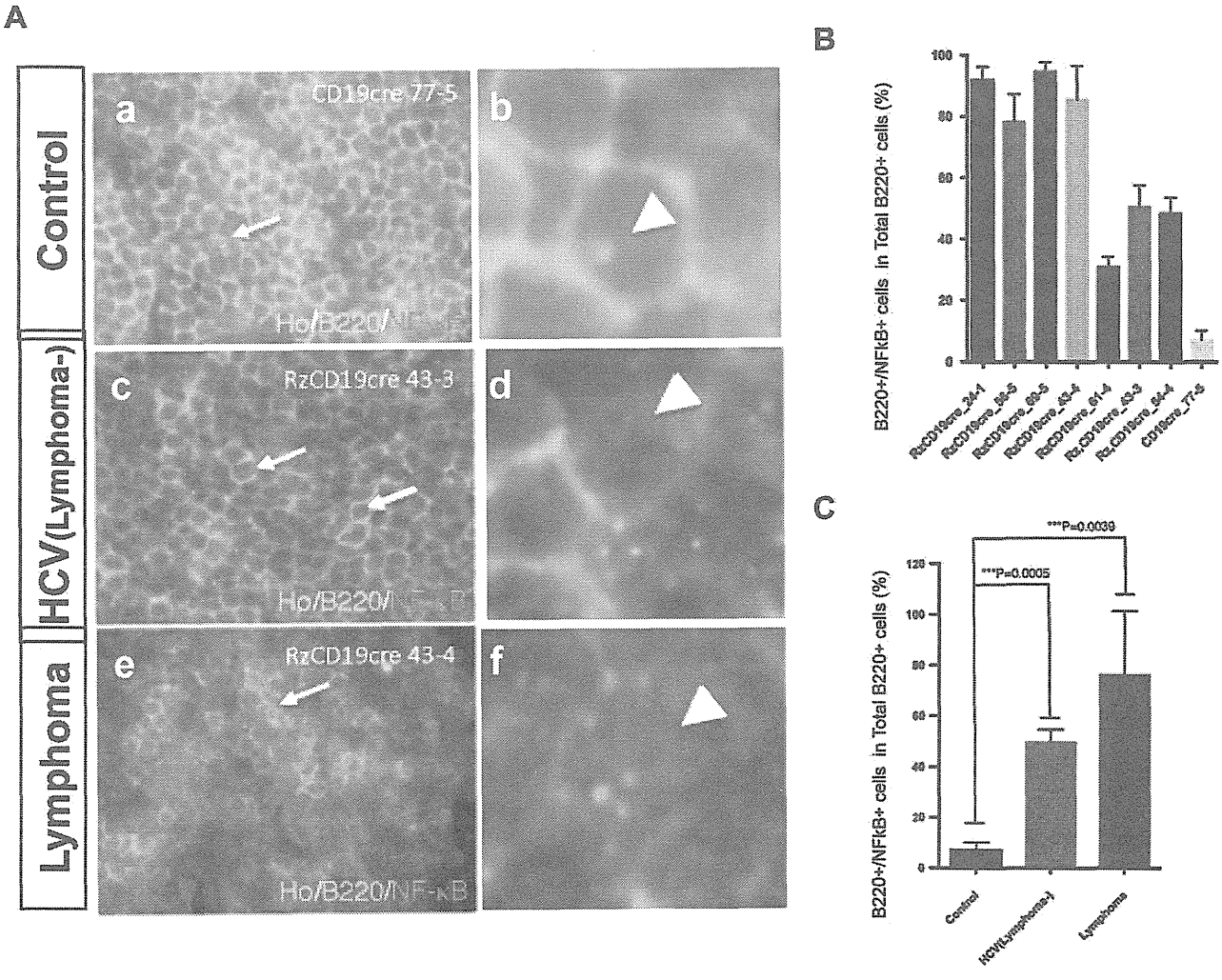

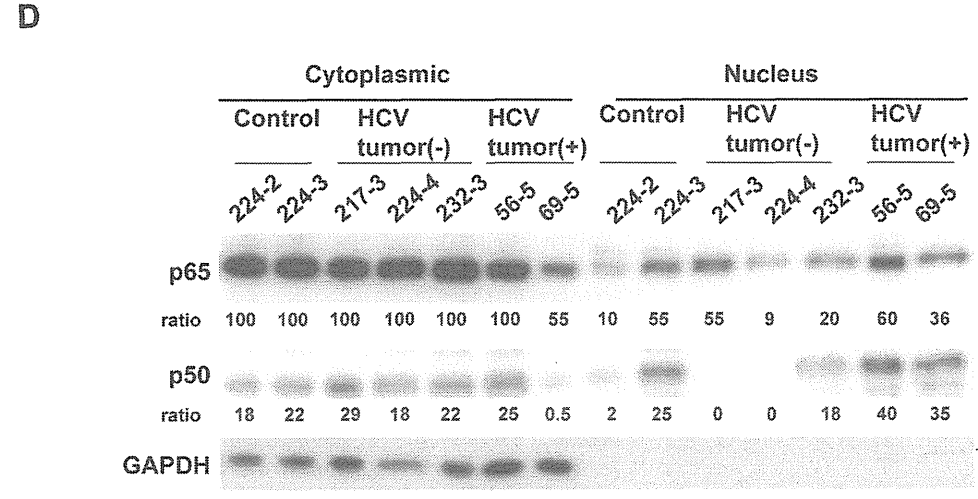

Figure 4. Double immunofluorescence localisation of B220 (Green) and NF-κB p65 (Red) in HCV-Tg mice and the fractionation analysis of mouse tissues. A: Co-localisation of NF-κB p65 immunoreactivity with B220 is indicated by arrows. (a–b) Cells double-positive for B220 and NF-κB in the control mouse (CD19cre). (c–d) Cells double-positive for B220 and NF-κB in the asymptomatic HCV-Tg mouse (RzCD19cre). (e–f) Cells double-positive for B220 and NF-κB in the lymphomatous HCV-Tg mouse (RzCD19cre). **B**: Quantitative analysis of the ratio of double-positive